Contact Mechanics and Elements of Tribology

Lecture 2.
Contact and Mechanics of Materials

Vladislav A. Yastrebov

Mines Paris - PSL, CNRS
Centre des Matériaux, Versailles, France

@ Centre des Matériaux (& virtually)
February 25, 2026

Interface physics

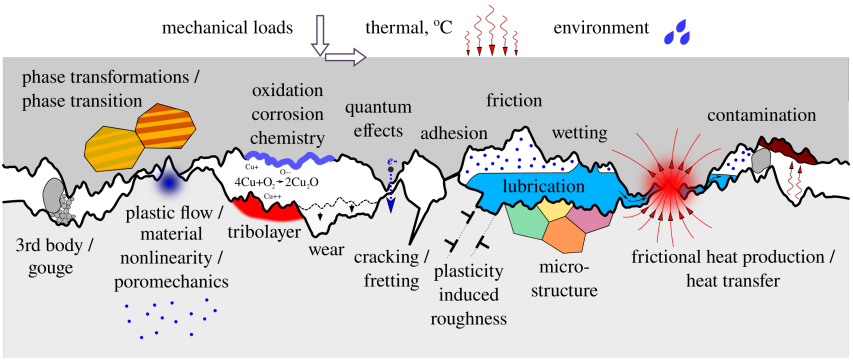

Tribological properties stem from this complex multi-scale physics of interfaces and near-surface layers[1]

[1] Vakis, Yastrebov, Scheibert, Nicola, Dini, Minfray,Almqvist, Paggi,Lee, Limbert, Molinari, Anciaux, Aghababaei, Echeverri Restrepo, Papangelo, Cammarata, Nicolini, Putignano, Carbone, Stupkiewicz, Lengiewicz, Costagliola, Bosia, Guarino, Pugno, Müser, Ciavarella, 2018. **Modeling and simulation in tribology across scales: An overview**. Tribology International, 125:169-199 (2018).

Outline

- Elastic-plastic contact
- Viscoelastic contact
- Frictional strengthening or time-dependent contact

Plasticity

Onset of plastic yielding

Hertz contact: body of revolution

- Onset of plasticity for max. pressure

$$p_Y = 1.6\sigma_Y$$

- Associated force

$$F_Y = \frac{1.6^3\pi^3R^2}{6}\left(\frac{\sigma_Y}{E^*}\right)^2\sigma_Y$$

- Associated contact radius

$$a_Y = \frac{1.6\pi R}{2}\frac{\sigma_Y}{E^*}$$

- Plastic flow starts at the depth

$$z_Y \approx 1.21R\frac{\sigma_Y}{E^*}$$

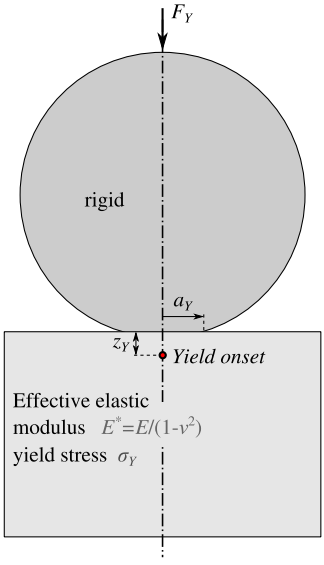

Elasto-plastic transition in contact

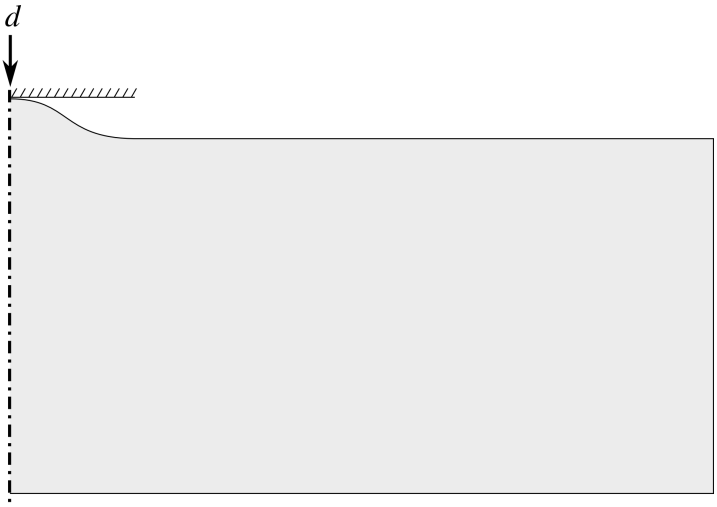

Elasto-plastic transition in contact

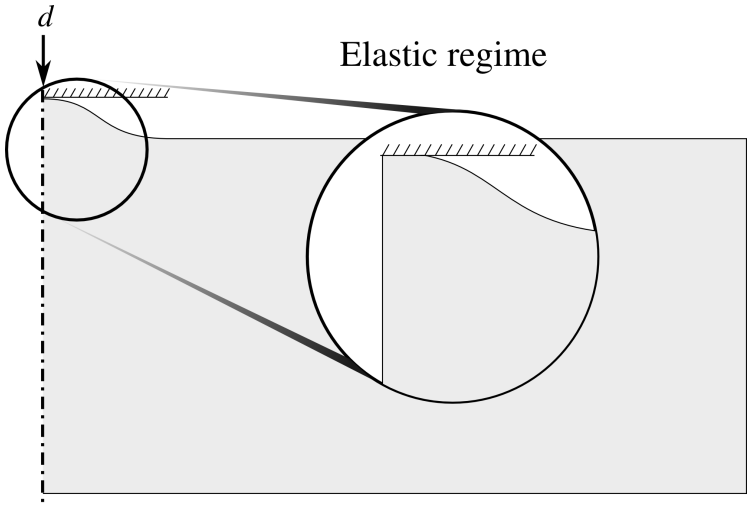

Elasto-plastic transition in contact

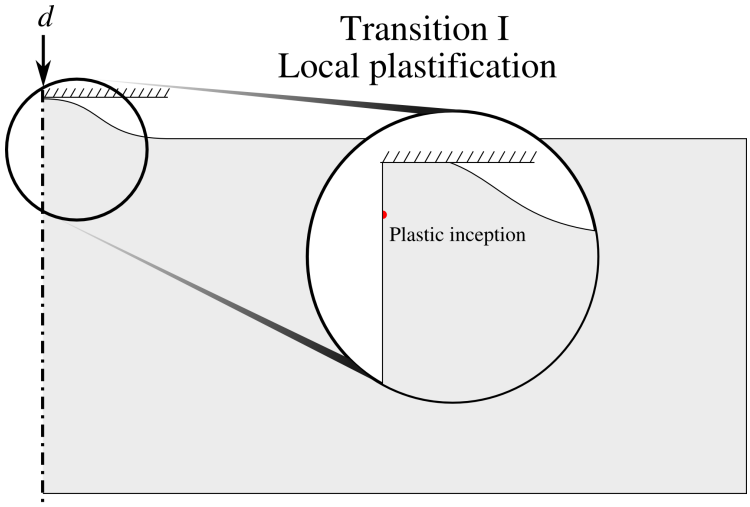

Elasto-plastic transition in contact

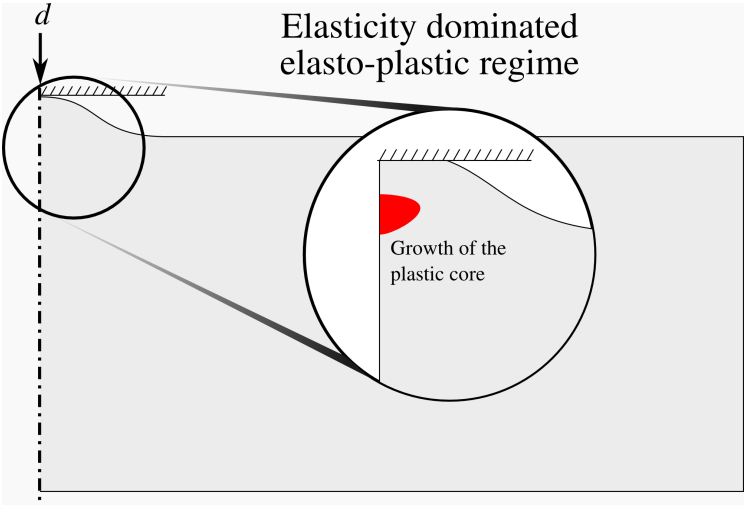

Elasto-plastic transition in contact

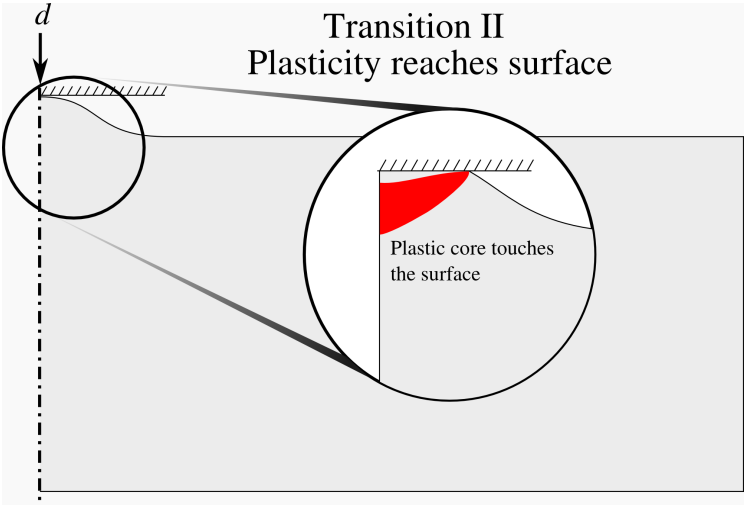

Elasto-plastic transition in contact

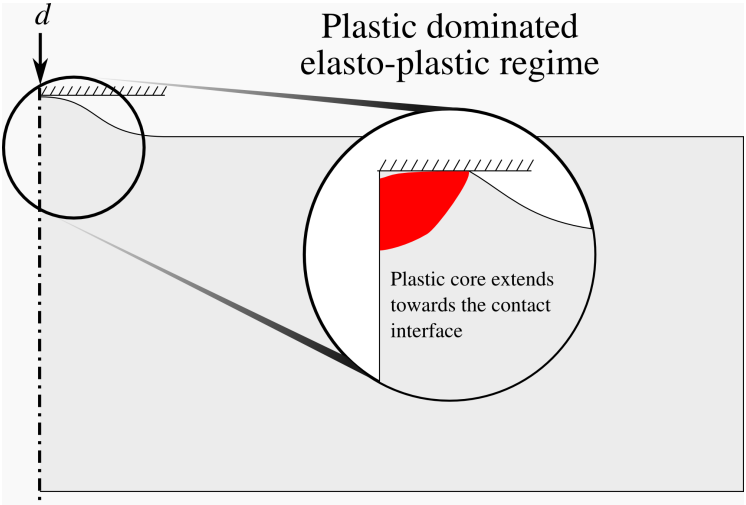

Elasto-plastic transition in contact

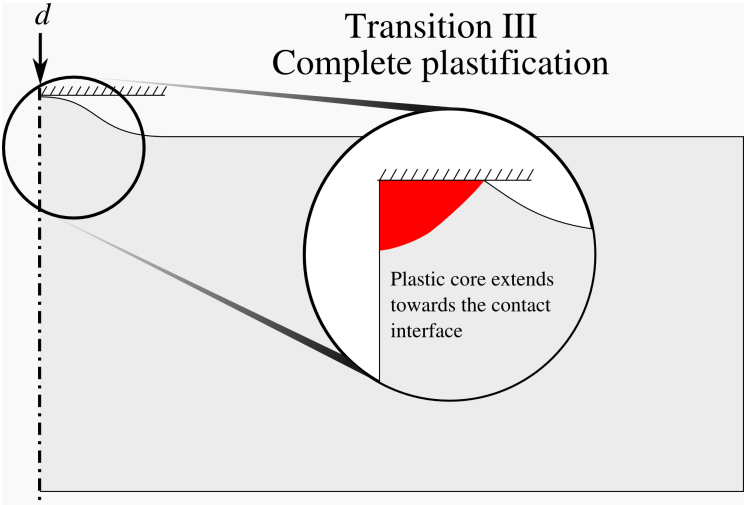

Elasto-plastic transition in contact

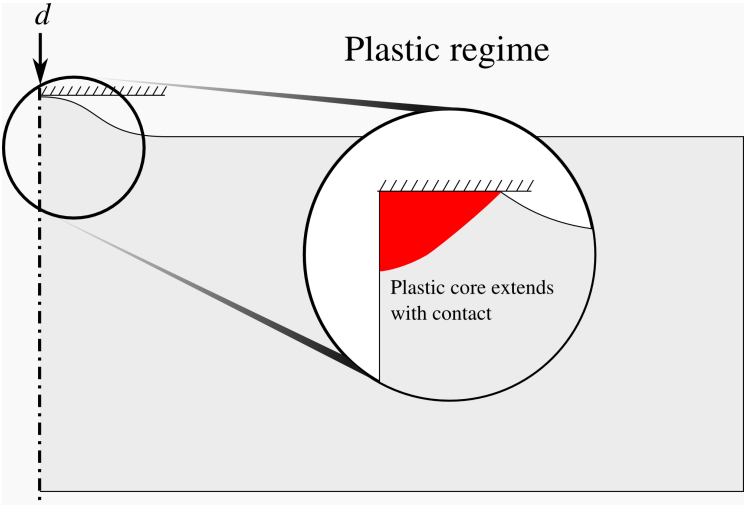

Elasto-plastic transition in contact

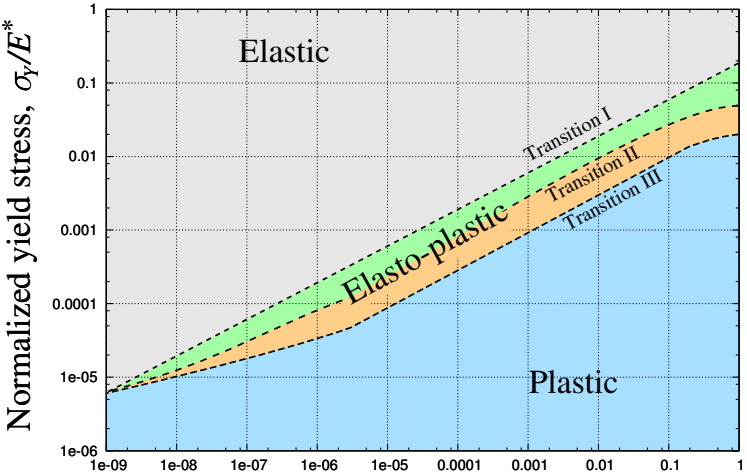

Deformation map for a sinusoidal asperity constructed with M. Liu, H. Proudhon

$h/\lambda = 0.1$

Elasto-plastic transition in contact

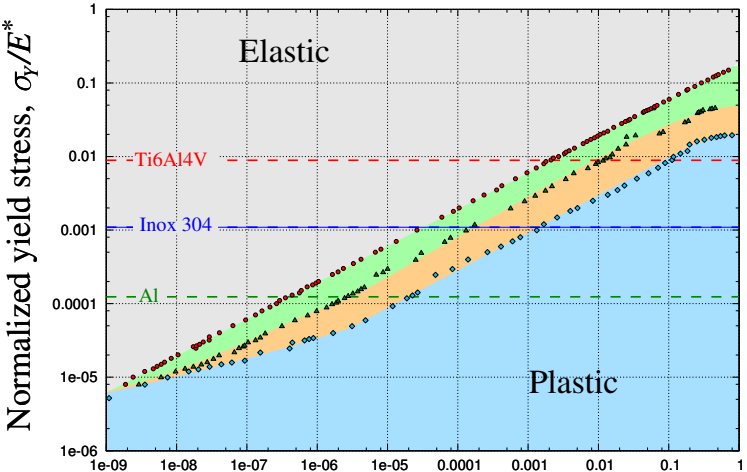

Deformation map for a sinusoidal asperity constructed with M. Liu, H. Proudhon

Elasto-plastic transition in contact

Case: $\sigma_Y/E = 0.0005$

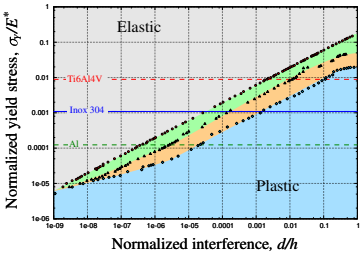

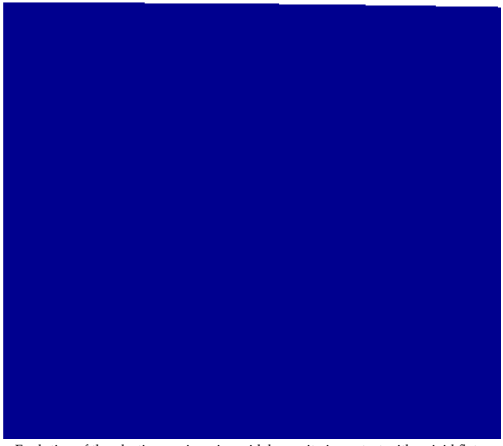

Evolution of the plastic zone in a sinusoidal asperity in contact with a rigid flat

Elasto-plastic transition in contact

Case: $\sigma_Y/E = 0.0005$

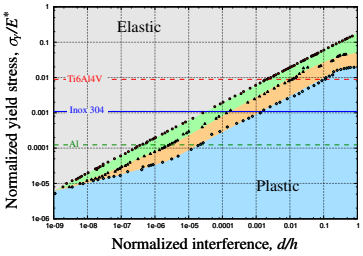

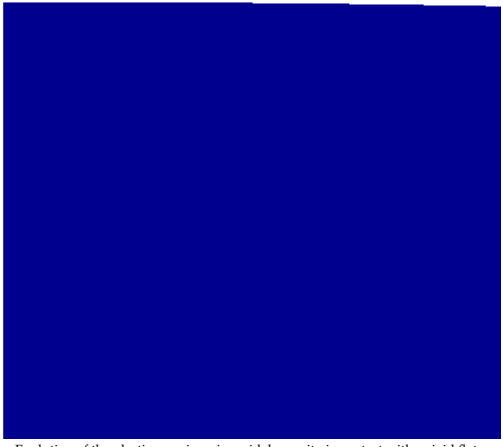

Evolution of the plastic zone in a sinusoidal asperity in contact with a rigid flat

Elasto-plastic transition in contact

Case: $\sigma_Y/E = 0.0005$

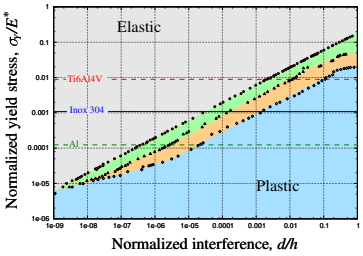

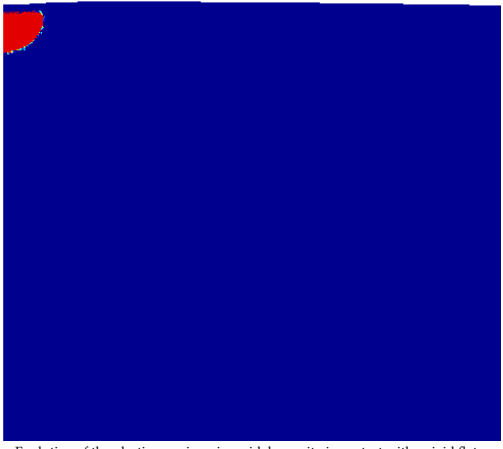

Evolution of the plastic zone in a sinusoidal asperity in contact with a rigid flat

Elasto-plastic transition in contact

Case: $\sigma_Y/E = 0.0005$

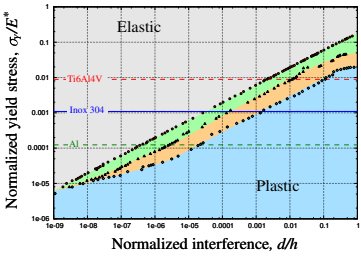

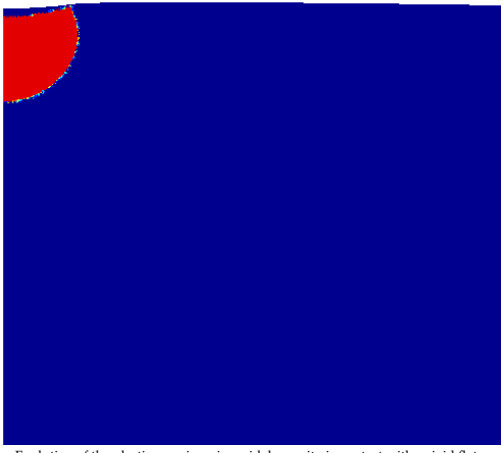

Evolution of the plastic zone in a sinusoidal asperity in contact with a rigid flat

Elasto-plastic transition in contact

Case: $\sigma_Y/E = 0.0005$

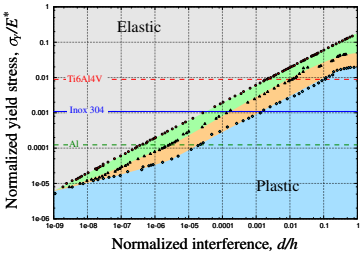

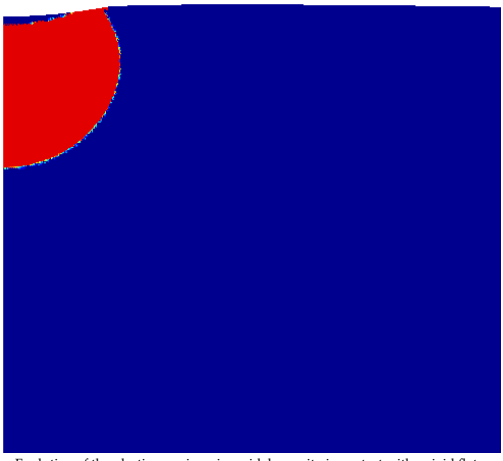

Evolution of the plastic zone in a sinusoidal asperity in contact with a rigid flat

Elasto-plastic transition in contact

Case: $\sigma_Y/E = 0.0005$

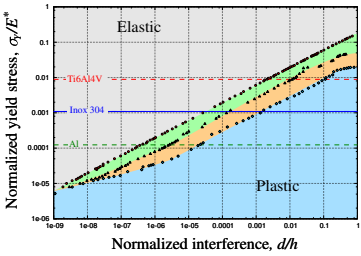

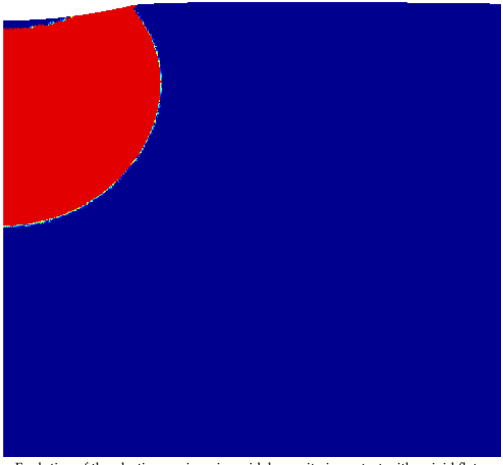

Evolution of the plastic zone in a sinusoidal asperity in contact with a rigid flat

Elasto-plastic transition in contact

Case: $\sigma_Y/E = 0.0005$

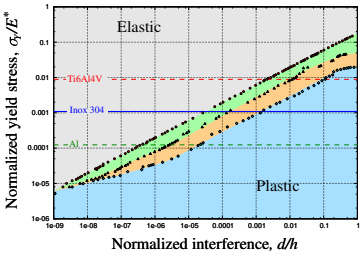

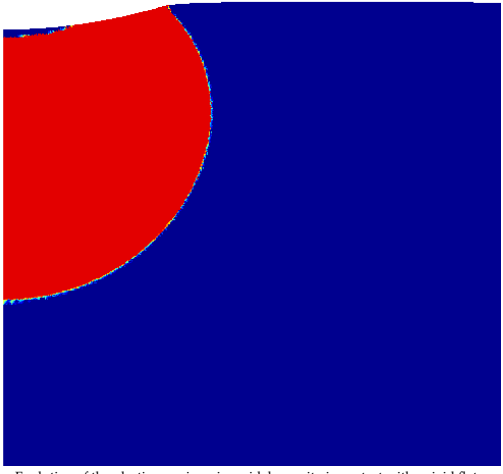

Evolution of the plastic zone in a sinusoidal asperity in contact with a rigid flat

Elasto-plastic transition in contact

Case: $\sigma_Y/E = 0.0005$

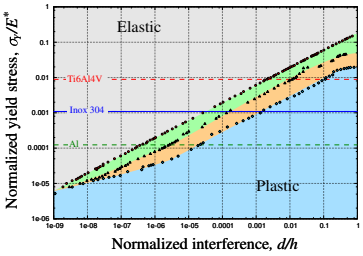

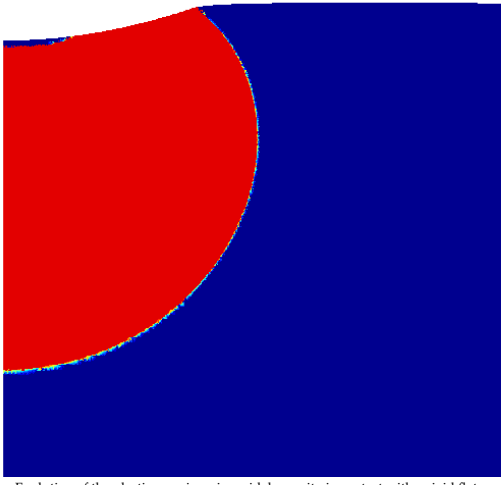

Evolution of the plastic zone in a sinusoidal asperity in contact with a rigid flat

Elastic-plastic normal contact: hardness

- Hardness ~ saturated plastic contact
- Recall: Vickers hardness $HV = N/A$
- Similarity solution[1]

$$\frac{N}{\pi a^2 \sigma_Y} = F\left(\frac{a}{R}\frac{E}{\sigma_y}\right)$$

- Hardness $H \approx 3\sigma_Y$

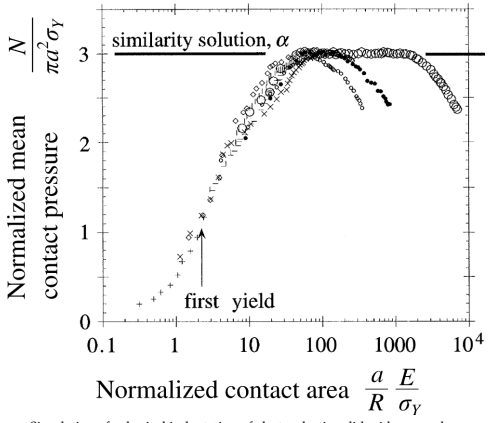

Simulation of spherical indentation of elasto-plastic solid with power-law hardening[2]

[1] Hill R., Storøakers B., Zdunek A.B. A theoretical study of the Brinell hardness test. Proc R Soc Lond A 436 (1989)

[2] Tabor, D. The Hardness of Metals. Oxford at the Clarendon Press (2000).

[3] Mesarovic S., N. Fleck, Spherical Indentation of Elastic-Plastic Solids, Proc R Soc Lond A 455 (1999)

Elasto-plastic contact under cyclic load

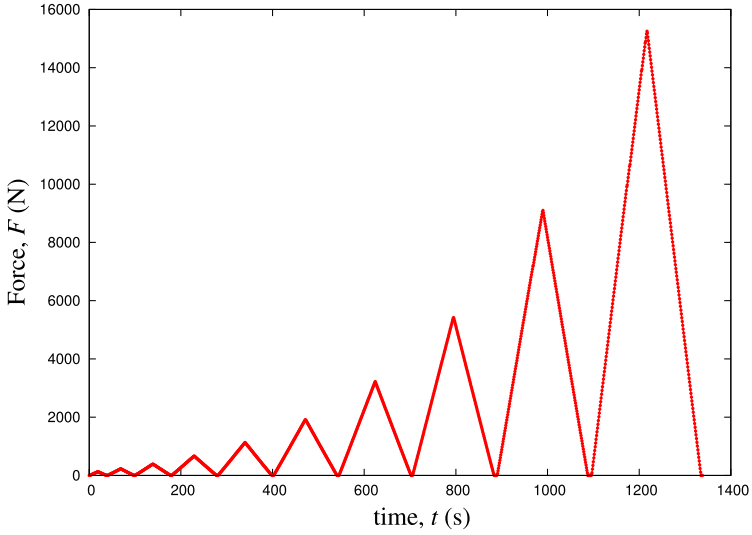

Elasto-plastic contact under cyclic load

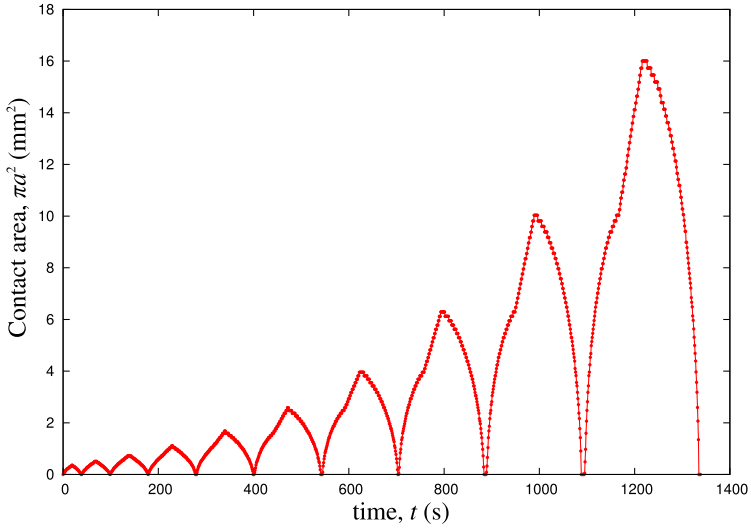

Elasto-plastic contact under cyclic load

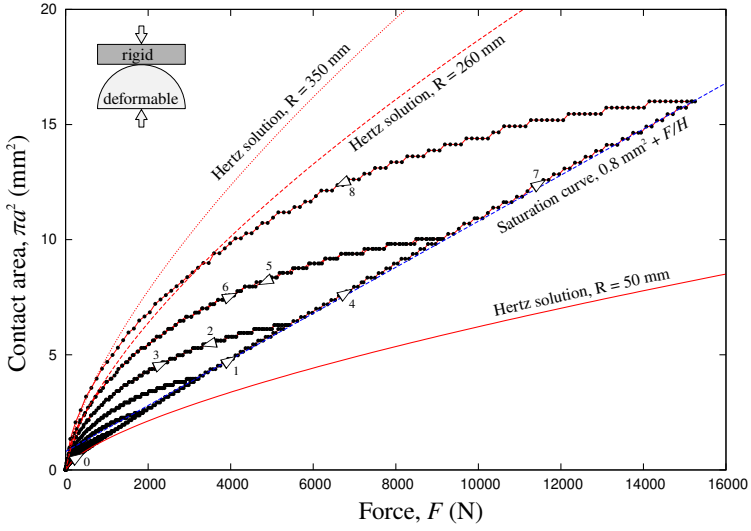

Elasto-plastic contact under cyclic load

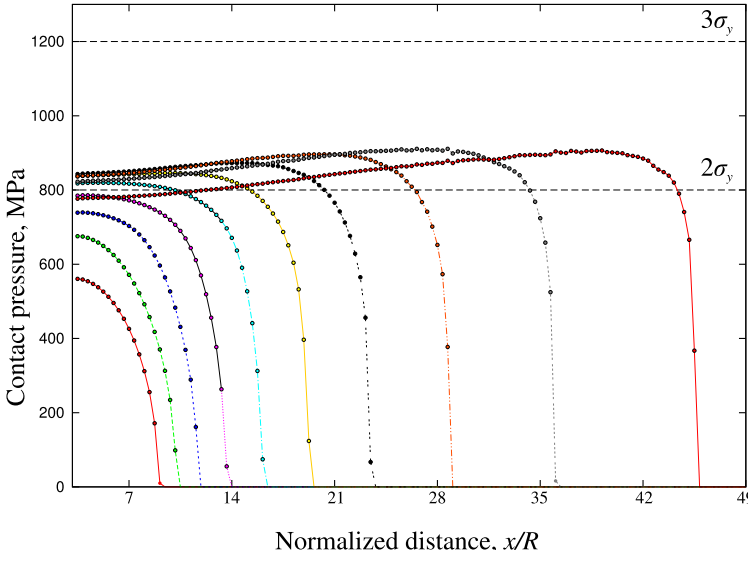

Elasto-plastic contact under cyclic load

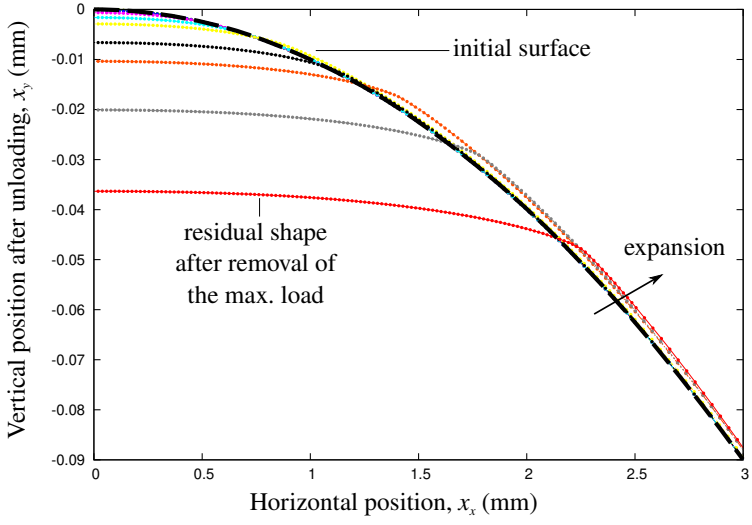

Finer-mesh and hardening effect

Two hardening models

- perfect plasticity $R = R_0$
- non-linear hardening with saturation $R(p) = R_0 + Q(1 - \exp(-bp))$

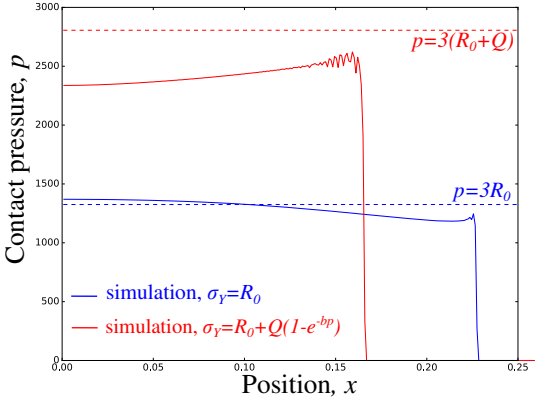

Finer-mesh and hardening effect

Two hardening models

- perfect plasticity $R = R_0$
- non-linear hardening with saturation $R(p) = R_0 + Q(1 - \exp(-bp))$

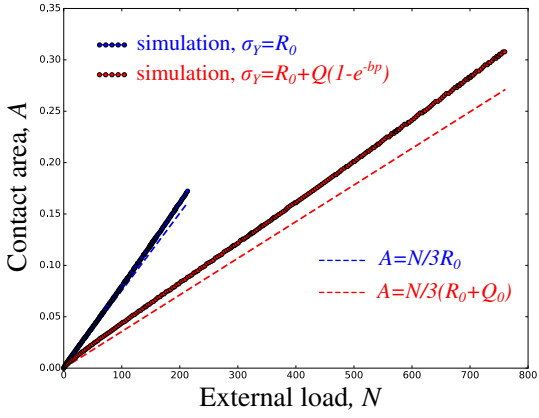

Deformation in fully plastic regime

✓ **Mesh effect**

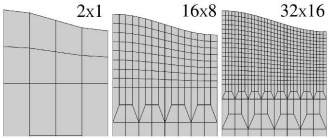

Shape effect

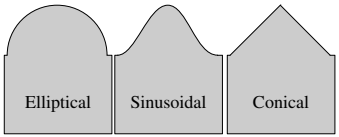

Edge effect

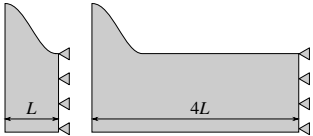

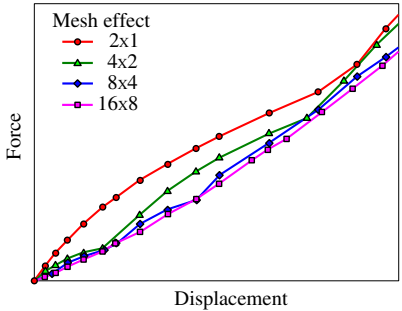

[1] V. A. Yastrebov, J. Durand, H. Proudhon, G. Cailletaud, CR Mecan, 339:473-490 (2011)

Deformation in fully plastic regime

Mesh effect

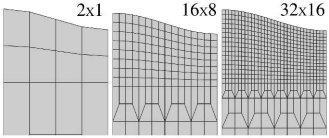

✓ **Shape effect**

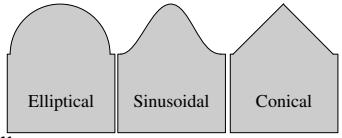

Edge effect

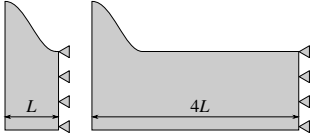

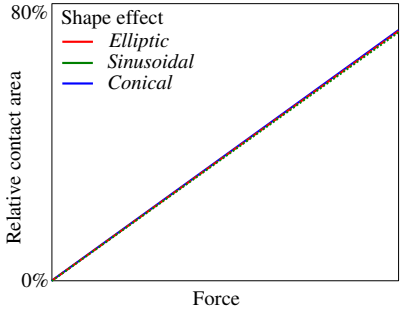

[1] V. A. Yastrebov, J. Durand, H. Proudhon, G. Cailletaud, CR Mecan, 339:473-490 (2011)

Deformation in fully plastic regime

Mesh effect

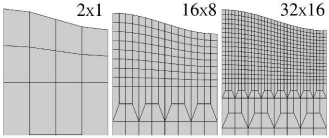

Shape effect

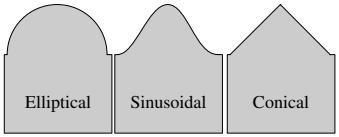

✓ **Edge effect**

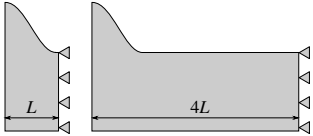

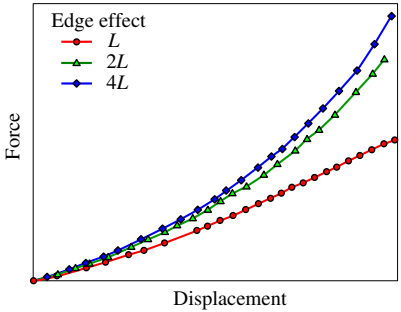

[1] V. A. Yastrebov, J. Durand, H. Proudhon, G. Cailletaud, CR Mecan, 339:473-490 (2011)

Near-surface vs bulk deformation

Material aspects

- Cold worked surface + recrystallized:
  smaller grains near the surface, Hall-Petch effect
- Thin coating films:
  nanograined, confined plasticity, Hall-Petch effect
- Oxides:
  brittle hard films

Geometrical aspects

- Roughness of all nature
- Indentation by asperities:
  confined plastic zone, high plastic strain gradients

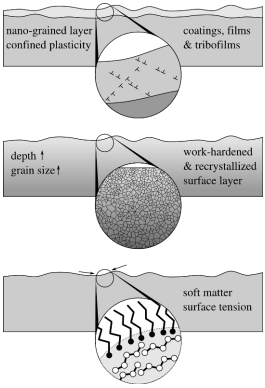

Onset of yielding at atomic scale

Hertz contact: body of revolution

- Onset of plasticity for pressure

$$p_Y = 1.6\sigma_Y$$

- Associated force

$$F_Y = \frac{1.6^3\pi^3R^2}{6}\left(\frac{\sigma_Y}{E^*}\right)^2\sigma_Y$$

- Associated contact radius

$$a_Y = \frac{1.6\pi R}{2}\frac{\sigma_Y}{E^*}$$

- Plastic flow starts at the depth

$$z_Y \approx 1.21R\frac{\sigma_Y}{E^*}$$

- Example: golden asperity

$E^* \approx 96$ GPa, $\sigma_y \approx 140$ MPa, $d \approx 4.1$Å

$R = 10\ \mu$m

$$F_Y \approx 3.8\ \mu\text{N}, \quad z_Y \approx 18\text{ nm}, \quad a_Y \approx 36\text{ nm}$$

$$z_Y \approx 44d, \quad a_Y \approx 88d$$

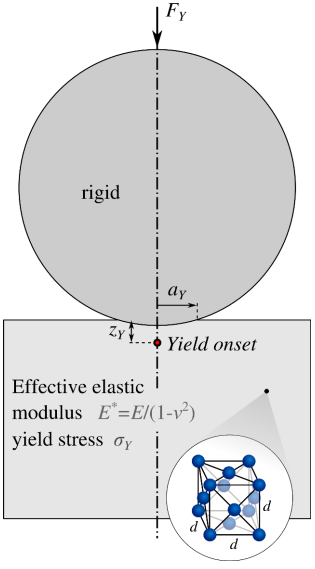

Onset of yielding at atomic scale

Hertz contact: body of revolution

- Onset of plasticity for pressure

$$p_Y = 1.6\sigma_Y$$

- Associated force

$$F_Y = \frac{1.6^3\pi^3R^2}{6}\left(\frac{\sigma_Y}{E^*}\right)^2\sigma_Y$$

- Associated contact radius

$$a_Y = \frac{1.6\pi R}{2}\frac{\sigma_Y}{E^*}$$

- Plastic flow starts at the depth

$$z_Y \approx 1.21R\frac{\sigma_Y}{E^*}$$

- Example: golden asperity

$E^* \approx 96$ GPa, $\sigma_y \approx 140$ MPa, $d \approx 4.1$Å

$R = 1\ \mu$m

$$F_Y \approx 38\text{ nN}, \quad z_Y \approx 1.8\text{ nm}, \quad a_Y \approx 3.6\text{ nm}$$

$$z_Y \approx 4.4d, \quad a_Y \approx 8.8d$$

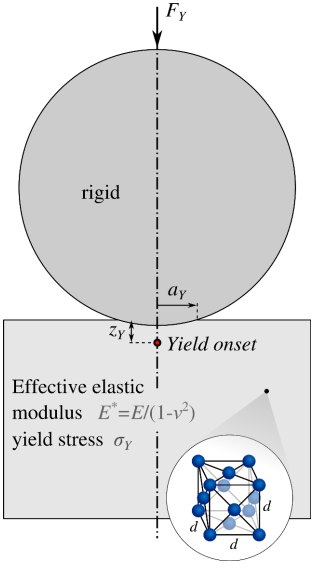

Indentation and hardness

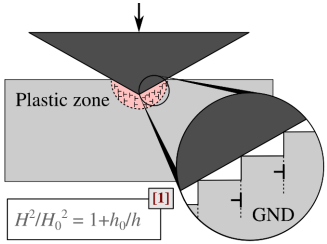

[1] Nix, Gao. *J Mech Phys Solids* (1998).

Indentation and hardness

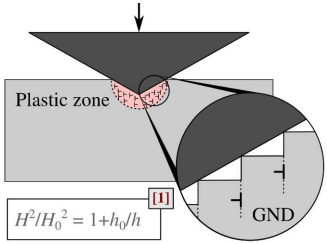

[1] Nix, Gao. *J Mech Phys Solids* (1998).
[2] Feng, Nix. *Scripta Mater* (2004).

Indentation and hardness

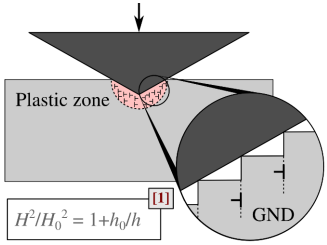

$$H^2/H_0^2 = 1+h_0/h \quad [1]$$

$$\frac{\text{Plastic zone } r}{\text{Contact radius } a} \sim 1 + b\exp(-h/h_1)$$

$$H^2/H_0^2 = 1+[1+b\exp(-h/h_1)]^{-3}h_0/h \quad [2]$$

$$(H-H_P)^2/(H_0-H_P)^2 = 1+[1+b\exp(-h/h_1)]^{-3}h_0/h \quad [2,3]$$

[1] Nix, Gao. *J Mech Phys Solids* (1998).
[2] Feng, Nix. *Scripta Mater* (2004).
[3] Qui, Huang, Nix, Hwang, Gao. *Acta Mater* (2001).

Indentation and hardness

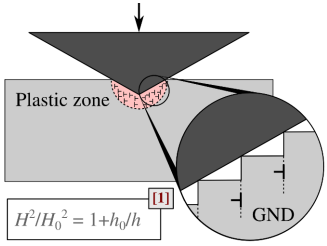

$H^2/H_0^2 = 1+h_0/h$ [1]

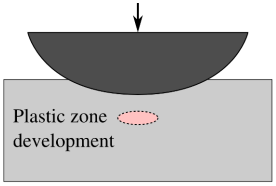

$$\frac{\text{Plastic zone } r}{\text{Contact radius } a} \sim 1 + b\exp(-h/h_1)$$

$H^2/H_0^2 = 1+[1+b\exp(-h/h_1)]^{-3}h_0/h$ [2]

$(H-H_P)^2/(H_0-H_P)^2 = 1+[1+b\exp(-h/h_1)]^{-3}h_0/h$ [2,3]

[1] Nix, Gao. *J Mech Phys Solids* (1998).
[2] Feng, Nix. *Scripta Mater* (2004).
[3] Qui, Huang, Nix, Hwang, Gao. *Acta Mater* (2001).

Indentation and hardness

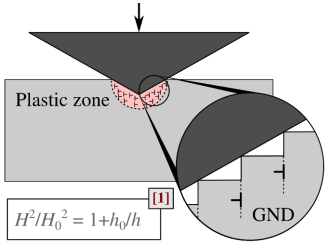

$$H^2/H_0^2 = 1+h_0/h \quad [1]$$

$$\frac{\text{Plastic zone } r}{\text{Contact radius } a} \sim 1 + b\exp(-h/h_1)$$

$$H^2/H_0^2 = 1+[1+b\exp(-h/h_1)]^{-3}h_0/h \quad [2]$$

$$(H-H_P)^2/(H_0-H_P)^2 = 1+[1+b\exp(-h/h_1)]^{-3}h_0/h \quad [2,3]$$

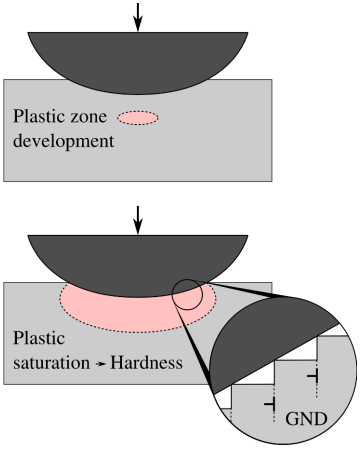

[1] Nix, Gao. *J Mech Phys Solids* (1998).
[2] Feng, Nix. *Scripta Mater* (2004).
[3] Qui, Huang, Nix, Hwang, Gao. *Acta Mater* (2001).

Indentation and hardness

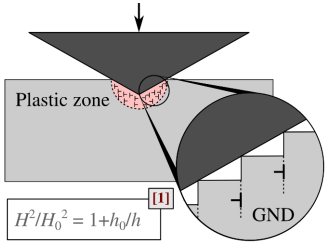

$H^2/H_0^2 = 1+h_0/h$ [1]

$$\frac{\text{Plastic zone } r}{\text{Contact radius } a} \sim 1 + b\exp(-h/h_1)$$

$H^2/H_0^2 = 1+[1+b\exp(-h/h_1)]^{-3}h_0/h$ [2]

$(H-H_P)^2/(H_0-H_P)^2 = 1+[1+b\exp(-h/h_1)]^{-3}h_0/h$ [2,3]

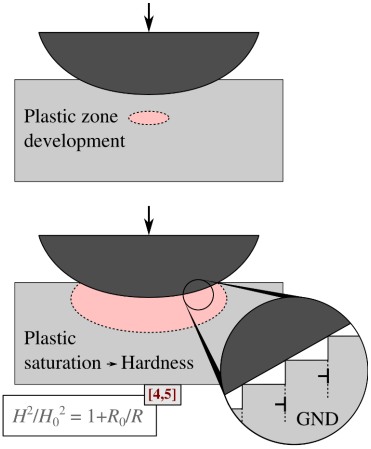

$H^2/H_0^2 = 1+R_0/R$ [4,5]

[1] Nix, Gao. *J Mech Phys Solids* (1998).
[2] Feng, Nix. *Scripta Mater* (2004).
[3] Qui, Huang, Nix, Hwang, Gao. *Acta Mater* (2001).
[4] Swadener, George, Pharr. *J Mech Phys Solids* (2002).
[5] Gao, Larson, Lee, Nicola, Tischler, Pharr. *J Appl Mech* (2015).

Enhanced material behavior: beyond *J2* plasticity

- Crystal plasticity models
  in indentation all slip systems are activated
  Difference with isotropic plasticity is small
- Discrete models with inherent characteristic length
  - *Molecular Dynamics*
  -*Dislocation Dynamics*
- Continuum models with characteristic length
  - *Cosserat continuum*[1]
  - *Second-gradient plasticity*[2]

[1] Forest S., Sievert R. Elastoviscoplastic constitutive frameworks for generalized continua. Acta Mech 160 (2003)

[2] Cordero N.M., Forest S. et al. Grain size effects on plastic strain and dislocation density tensor fields in metal polycrystals, Comp Mater Sci 52 (2012)

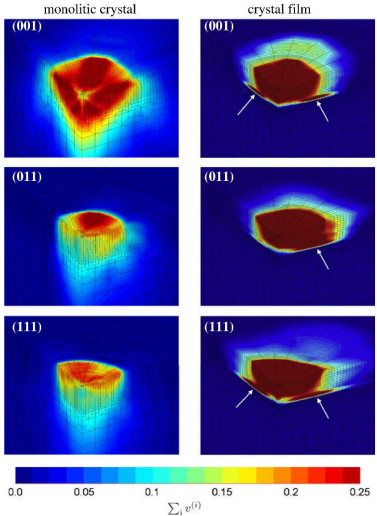

Spherical indentation of FCC copper crystal using crystal plasticity model in Zset

[3] Casals O., Forest S. Finite element crystal plasticity analysis of spherical indentation in bulk single crystals and coatings. Comp Mater Sci 45 (2009)

Enhanced material behavior: beyond *J2* plasticity

- Crystal plasticity models
  in indentation all slip systems are activated
  Difference with isotropic plasticity is small
- Discrete models with inherent characteristic length
  - *Molecular Dynamics*
  -*Dislocation Dynamics*
- Continuum models with characteristic length
  - *Cosserat continuum*[1]
  - *Second-gradient plasticity*[2]

[1] Forest S., Sievert R. Elastoviscoplastic constitutive frameworks for generalized continua. Acta Mech 160 (2003)

[2] Cordero N.M., Forest S. et al. Grain size effects on plastic strain and dislocation density tensor fields in metal polycrystals, Comp Mater Sci 52 (2012)

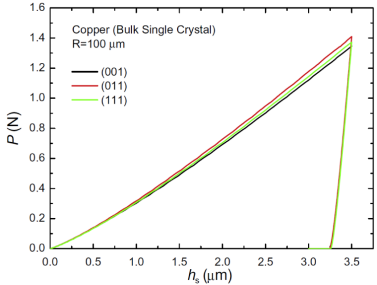

Spherical indentation of FCC copper crystal using crystal plasticity model in Zset

[3] Casals O., Forest S. Finite element crystal plasticity analysis of spherical indentation in bulk single crystals and coatings. Comp Mater Sci 45 (2009)

Enhanced material behavior: beyond *J2* plasticity

- Crystal plasticity models
  in indentation all slip systems are activated
  Difference with isotropic plasticity is small
- Discrete models with inherent characteristic length
  - *Molecular Dynamics*
  -*Dislocation Dynamics*
- Continuum models with characteristic length
  - *Cosserat continuum*[1]
  - *Second-gradient plasticity*[2]

[1] Forest S., Sievert R. Elastoviscoplastic constitutive frameworks for generalized continua. Acta Mech 160 (2003)

[2] Cordero N.M., Forest S. et al. Grain size effects on plastic strain and dislocation density tensor fields in metal polycrystals, Comp Mater Sci 52 (2012)

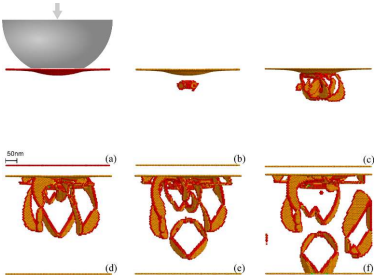

MD simulation of a spherical indentation on (111) FCC cube

[4] H.J. Chang, M. Fivel, D. Rodney, M. Verdier. Multiscale modelling of indentation in FCC metals: From atomic to continuum, CR Physique 11 (2010)

Enhanced material behavior: beyond *J2* plasticity

- Crystal plasticity models
  in indentation all slip systems are activated
  Difference with isotropic plasticity is small
- Discrete models with inherent characteristic length
  - *Molecular Dynamics*
  -*Dislocation Dynamics*
- Continuum models with characteristic length
  - *Cosserat continuum*[1]
  - *Second-gradient plasticity*[2]

[1] Forest S., Sievert R. Elastoviscoplastic constitutive frameworks for generalized continua. Acta Mech 160 (2003)

[2] Cordero N.M., Forest S. et al. Grain size effects on plastic strain and dislocation density tensor fields in metal polycrystals, Comp Mater Sci 52 (2012)

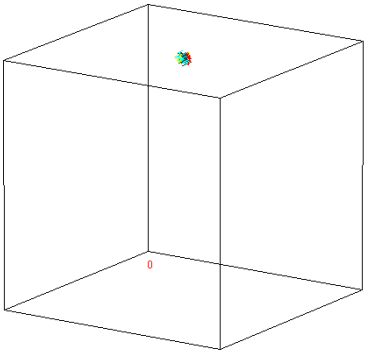

Resulting DD simulation of a spherical indentation on (111) FCC cube

[4] H.J. Chang, M. Fivel, D. Rodney, M. Verdier. Multiscale modelling of indentation in FCC metals: From atomic to continuum, CR Physique 11 (2010)

www.numodis.com

Enhanced material behavior: beyond *J2* plasticity

- Crystal plasticity models
  in indentation all slip systems are activated
  Difference with isotropic plasticity is small
- Discrete models with inherent characteristic length
  - *Molecular Dynamics*
  -*Dislocation Dynamics*
- Continuum models with characteristic length
  - *Cosserat continuum*[1]
  - *Second-gradient plasticity*[2]

[1] Forest S., Sievert R. Elastoviscoplastic constitutive frameworks for generalized continua. Acta Mech 160 (2003)

[2] Cordero N.M., Forest S. et al. Grain size effects on plastic strain and dislocation density tensor fields in metal polycrystals, Comp Mater Sci 52 (2012)

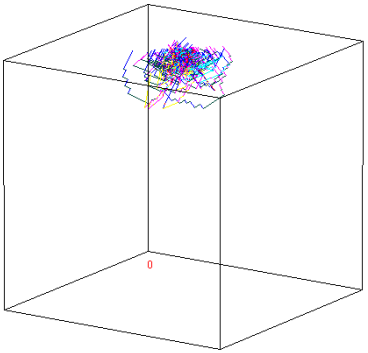

Resulting DD simulation of a spherical indentation on (111) FCC cube

[4] H.J. Chang, M. Fivel, D. Rodney, M. Verdier. Multiscale modelling of indentation in FCC metals: From atomic to continuum, CR Physique 11 (2010)

www.numodis.com

Enhanced material behavior: beyond *J2* plasticity

- Crystal plasticity models
  in indentation all slip systems are activated
  Difference with isotropic plasticity is small
- Discrete models with inherent characteristic length
  - *Molecular Dynamics*
  -*Dislocation Dynamics*
- Continuum models with characteristic length
  - *Cosserat continuum*[1]
  - *Second-gradient plasticity*[2]

[1] Forest S., Sievert R. Elastoviscoplastic constitutive frameworks for generalized continua. Acta Mech 160 (2003)

[2] Cordero N.M., Forest S. et al. Grain size effects on plastic strain and dislocation density tensor fields in metal polycrystals, Comp Mater Sci 52 (2012)

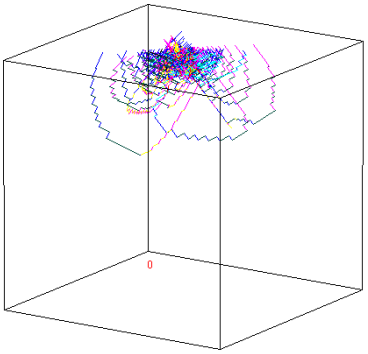

Resulting DD simulation of a spherical indentation on (111) FCC cube

[4] H.J. Chang, M. Fivel, D. Rodney, M. Verdier. Multiscale modelling of indentation in FCC metals: From atomic to continuum, CR Physique 11 (2010)

www.numodis.com

Enhanced material behavior: beyond *J2* plasticity

- Crystal plasticity models
  in indentation all slip systems are activated
  Difference with isotropic plasticity is small
- Discrete models with inherent characteristic length
  - *Molecular Dynamics*
  -*Dislocation Dynamics*
- Continuum models with characteristic length
  - *Cosserat continuum*[1]
  - *Second-gradient plasticity*[2]

[1] Forest S., Sievert R. Elastoviscoplastic constitutive frameworks for generalized continua. Acta Mech 160 (2003)

[2] Cordero N.M., Forest S. et al. Grain size effects on plastic strain and dislocation density tensor fields in metal polycrystals, Comp Mater Sci 52 (2012)

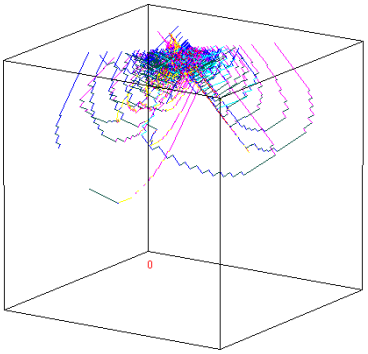

Resulting DD simulation of a spherical indentation on (111) FCC cube

[4] H.J. Chang, M. Fivel, D. Rodney, M. Verdier. Multiscale modelling of indentation in FCC metals: From atomic to continuum, CR Physique 11 (2010)

www.numodis.com

Enhanced material behavior: beyond *J2* plasticity

- Crystal plasticity models
  in indentation all slip systems are activated
  Difference with isotropic plasticity is small
- Discrete models with inherent characteristic length
  - *Molecular Dynamics*
  -*Dislocation Dynamics*
- Continuum models with characteristic length
  - *Cosserat continuum*[1]
  - *Second-gradient plasticity*[2]

[1] Forest S., Sievert R. Elastoviscoplastic constitutive frameworks for generalized continua. Acta Mech 160 (2003)

[2] Cordero N.M., Forest S. et al. Grain size effects on plastic strain and dislocation density tensor fields in metal polycrystals, Comp Mater Sci 52 (2012)

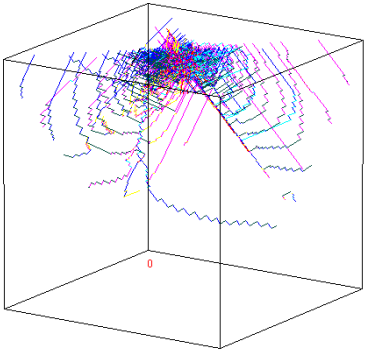

Resulting DD simulation of a spherical indentation on (111) FCC cube

[4] H.J. Chang, M. Fivel, D. Rodney, M. Verdier. Multiscale modelling of indentation in FCC metals: From atomic to continuum, CR Physique 11 (2010)

www.numodis.com

Enhanced material behavior: beyond *J2* plasticity

- Crystal plasticity models
  in indentation all slip systems are activated
  Difference with isotropic plasticity is small
- Discrete models with inherent characteristic length
  - *Molecular Dynamics*
  -*Dislocation Dynamics*
- Continuum models with characteristic length
  - *Cosserat continuum*[1]
  - *Second-gradient plasticity*[2]

[1] Forest S., Sievert R. Elastoviscoplastic constitutive frameworks for generalized continua. Acta Mech 160 (2003)

[2] Cordero N.M., Forest S. et al. Grain size effects on plastic strain and dislocation density tensor fields in metal polycrystals, Comp Mater Sci 52 (2012)

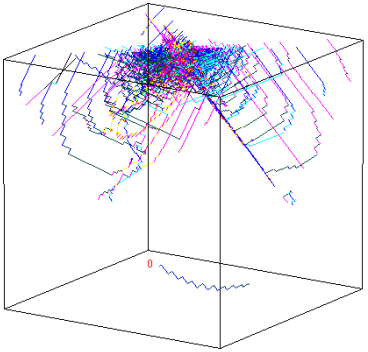

Resulting DD simulation of a spherical indentation on (111) FCC cube

[4] H.J. Chang, M. Fivel, D. Rodney, M. Verdier. Multiscale modelling of indentation in FCC metals: From atomic to continuum, CR Physique 11 (2010)

www.numodis.com

Enhanced material behavior: beyond *J2* plasticity

- Crystal plasticity models
  in indentation all slip systems are activated
  Difference with isotropic plasticity is small
- Discrete models with inherent characteristic length
  - *Molecular Dynamics*
  -*Dislocation Dynamics*
- Continuum models with characteristic length
  - *Cosserat continuum*[1]
  - *Second-gradient plasticity*[2]

[1] Forest S., Sievert R. Elastoviscoplastic constitutive frameworks for generalized continua. Acta Mech 160 (2003)

[2] Cordero N.M., Forest S. et al. Grain size effects on plastic strain and dislocation density tensor fields in metal polycrystals, Comp Mater Sci 52 (2012)

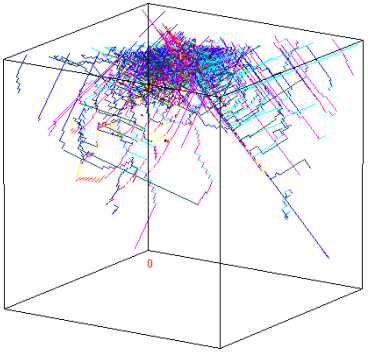

Resulting DD simulation of a spherical indentation on (111) FCC cube

[4] H.J. Chang, M. Fivel, D. Rodney, M. Verdier. Multiscale modelling of indentation in FCC metals: From atomic to continuum, CR Physique 11 (2010)

www.numodis.com

Enhanced material behavior: beyond *J2* plasticity

- Crystal plasticity models
  in indentation all slip systems are activated
  Difference with isotropic plasticity is small
- Discrete models with inherent characteristic length
  - *Molecular Dynamics*
  -*Dislocation Dynamics*
- Continuum models with characteristic length
  - *Cosserat continuum*[1]
  - *Second-gradient plasticity*[2]

[1] Forest S., Sievert R. Elastoviscoplastic constitutive frameworks for generalized continua. Acta Mech 160 (2003)

[2] Cordero N.M., Forest S. et al. Grain size effects on plastic strain and dislocation density tensor fields in metal polycrystals, Comp Mater Sci 52 (2012)

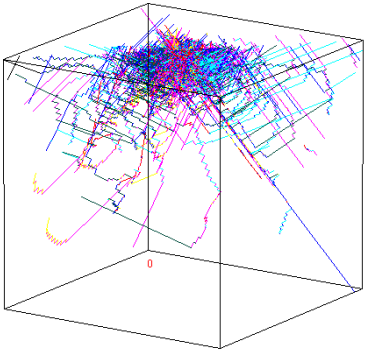

Resulting DD simulation of a spherical indentation on (111) FCC cube

[4] H.J. Chang, M. Fivel, D. Rodney, M. Verdier. Multiscale modelling of indentation in FCC metals: From atomic to continuum, CR Physique 11 (2010)

www.numodis.com

Enhanced material behavior: beyond *J2* plasticity

- Crystal plasticity models
  in indentation all slip systems are activated
  Difference with isotropic plasticity is small
- Discrete models with inherent characteristic length
  - *Molecular Dynamics*
  -*Dislocation Dynamics*
- Continuum models with characteristic length
  - *Cosserat continuum*[1]
  - *Second-gradient plasticity*[2]

[1] Forest S., Sievert R. Elastoviscoplastic constitutive frameworks for generalized continua. Acta Mech 160 (2003)

[2] Cordero N.M., Forest S. et al. Grain size effects on plastic strain and dislocation density tensor fields in metal polycrystals, Comp Mater Sci 52 (2012)

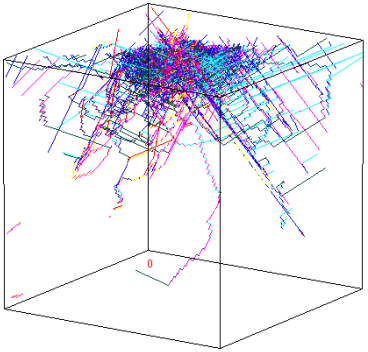

Resulting DD simulation of a spherical indentation on (111) FCC cube

[4] H.J. Chang, M. Fivel, D. Rodney, M. Verdier. Multiscale modelling of indentation in FCC metals: From atomic to continuum, CR Physique 11 (2010)

www.numodis.com

Enhanced material behavior: beyond *J2* plasticity

- Crystal plasticity models
  in indentation all slip systems are activated
  Difference with isotropic plasticity is small
- Discrete models with inherent characteristic length
  - *Molecular Dynamics*
  -*Dislocation Dynamics*
- Continuum models with characteristic length
  - *Cosserat continuum*[1]
  - *Second-gradient plasticity*[2]

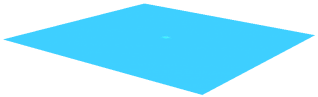

DD simulation of Berkovich nanoindentation

www.numodis.com

[1] Forest S., Sievert R. Elastoviscoplastic constitutive frameworks for generalized continua. Acta Mech 160 (2003)

[2] Cordero N.M., Forest S. et al. Grain size effects on plastic strain and dislocation density tensor fields in metal polycrystals, Comp Mater Sci 52 (2012)

Enhanced material behavior: beyond *J2* plasticity

- Crystal plasticity models
  in indentation all slip systems are activated
  Difference with isotropic plasticity is small
- Discrete models with inherent characteristic length
  - *Molecular Dynamics*
  -*Dislocation Dynamics*
- Continuum models with characteristic length
  - *Cosserat continuum*[1]
  - *Second-gradient plasticity*[2]

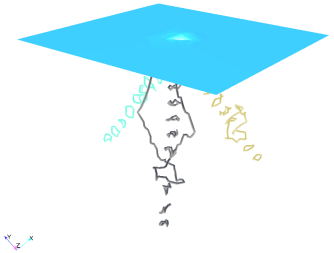

DD simulation of Berkovich nanoindentation

www.numodis.com

[1] Forest S., Sievert R. Elastoviscoplastic constitutive frameworks for generalized continua. Acta Mech 160 (2003)

[2] Cordero N.M., Forest S. et al. Grain size effects on plastic strain and dislocation density tensor fields in metal polycrystals, Comp Mater Sci 52 (2012)

Enhanced material behavior: beyond *J2* plasticity

- Crystal plasticity models
  in indentation all slip systems are activated
  Difference with isotropic plasticity is small
- Discrete models with inherent characteristic length
  - *Molecular Dynamics*
  -*Dislocation Dynamics*
- Continuum models with characteristic length
  - *Cosserat continuum*[1]
  - *Second-gradient plasticity*[2]

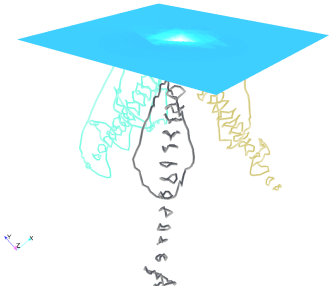

DD simulation of Berkovich nanoindentation

www.numodis.com

[1] Forest S., Sievert R. Elastoviscoplastic constitutive frameworks for generalized continua. Acta Mech 160 (2003)

[2] Cordero N.M., Forest S. et al. Grain size effects on plastic strain and dislocation density tensor fields in metal polycrystals, Comp Mater Sci 52 (2012)

Enhanced material behavior: beyond *J2* plasticity

- Crystal plasticity models
  in indentation all slip systems are activated
  Difference with isotropic plasticity is small
- Discrete models with inherent characteristic length
  - *Molecular Dynamics*
  -*Dislocation Dynamics*
- Continuum models with characteristic length
  - *Cosserat continuum*[1]
  - *Second-gradient plasticity*[2]

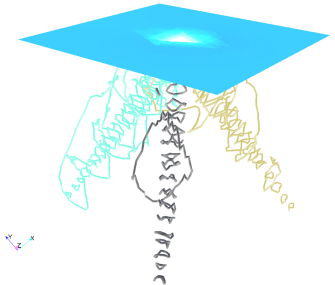

DD simulation of Berkovich nanoindentation

www.numodis.com

[1] Forest S., Sievert R. Elastoviscoplastic constitutive frameworks for generalized continua. Acta Mech 160 (2003)

[2] Cordero N.M., Forest S. et al. Grain size effects on plastic strain and dislocation density tensor fields in metal polycrystals, Comp Mater Sci 52 (2012)

Enhanced material behavior: beyond *J2* plasticity

- Crystal plasticity models
  in indentation all slip systems are activated
  Difference with isotropic plasticity is small
- Discrete models with inherent characteristic length
  - *Molecular Dynamics*
  -*Dislocation Dynamics*
- Continuum models with characteristic length
  - *Cosserat continuum*[1]
  - *Second-gradient plasticity*[2]

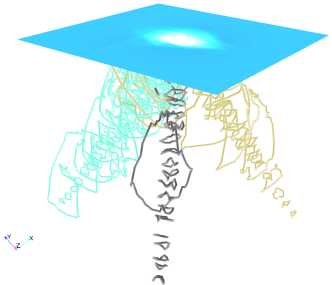

DD simulation of Berkovich nanoindentation

www.numodis.com

[1] Forest S., Sievert R. Elastoviscoplastic constitutive frameworks for generalized continua. Acta Mech 160 (2003)

[2] Cordero N.M., Forest S. et al. Grain size effects on plastic strain and dislocation density tensor fields in metal polycrystals, Comp Mater Sci 52 (2012)

Enhanced material behavior: beyond *J2* plasticity

- Crystal plasticity models
  in indentation all slip systems are activated
  Difference with isotropic plasticity is small
- Discrete models with inherent characteristic length
  - *Molecular Dynamics*
  -*Dislocation Dynamics*
- Continuum models with characteristic length
  - *Cosserat continuum*[1]
  - *Second-gradient plasticity*[2]

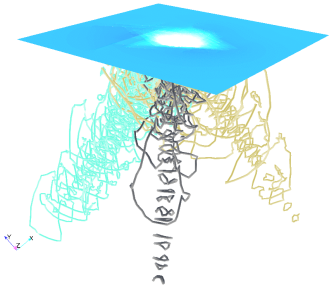

DD simulation of Berkovich nanoindentation

www.numodis.com

[1] Forest S., Sievert R. Elastoviscoplastic constitutive frameworks for generalized continua. Acta Mech 160 (2003)

[2] Cordero N.M., Forest S. et al. Grain size effects on plastic strain and dislocation density tensor fields in metal polycrystals, Comp Mater Sci 52 (2012)

Enhanced material behavior: beyond *J2* plasticity

- Crystal plasticity models
  in indentation all slip systems are activated
  Difference with isotropic plasticity is small
- Discrete models with inherent characteristic length
  - *Molecular Dynamics*
  -*Dislocation Dynamics*
- Continuum models with characteristic length
  - *Cosserat continuum*[1]
  - *Second-gradient plasticity*[2]

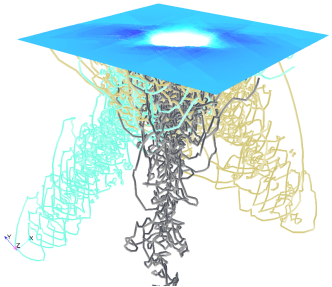

DD simulation of Berkovich nanoindentation

www.numodis.com

[1] Forest S., Sievert R. Elastoviscoplastic constitutive frameworks for generalized continua. Acta Mech 160 (2003)

[2] Cordero N.M., Forest S. et al. Grain size effects on plastic strain and dislocation density tensor fields in metal polycrystals, Comp Mater Sci 52 (2012)

Enhanced material behavior: beyond *J2* plasticity

- Crystal plasticity models
  in indentation all slip systems are activated
  Difference with isotropic plasticity is small
- Discrete models with inherent characteristic length
  - *Molecular Dynamics*
  -*Dislocation Dynamics*
- Continuum models with characteristic length
  - *Cosserat continuum*[1]
  - *Second-gradient plasticity*[2]

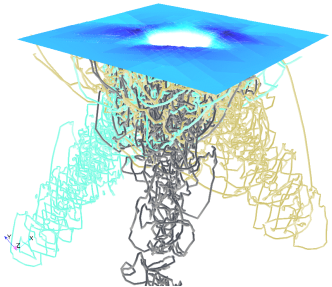

DD simulation of Berkovich nanoindentation

www.numodis.com

[1] Forest S., Sievert R. Elastoviscoplastic constitutive frameworks for generalized continua. Acta Mech 160 (2003)

[2] Cordero N.M., Forest S. et al. Grain size effects on plastic strain and dislocation density tensor fields in metal polycrystals, Comp Mater Sci 52 (2012)

Enhanced material behavior: beyond *J2* plasticity

- Crystal plasticity models
  in indentation all slip systems are activated
  Difference with isotropic plasticity is small
- Discrete models with inherent characteristic length
  - *Molecular Dynamics*
  -*Dislocation Dynamics*
- Continuum models with characteristic length
  - *Cosserat continuum*[1]
  - *Second-gradient plasticity*[2]

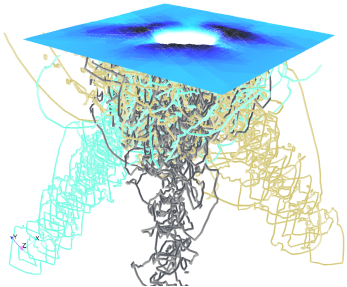

DD simulation of Berkovich nanoindentation

www.numodis.com

[1] Forest S., Sievert R. Elastoviscoplastic constitutive frameworks for generalized continua. Acta Mech 160 (2003)

[2] Cordero N.M., Forest S. et al. Grain size effects on plastic strain and dislocation density tensor fields in metal polycrystals, Comp Mater Sci 52 (2012)

Cosserat continuum

- Field variables (displacement & rotation): $\underline{u}, \underline{\omega}$
- Small deformation tensor: $\underline{\underline{\varepsilon}} = \nabla \underline{u} + {}^3\underline{\underline{\epsilon}} \cdot \underline{\omega}$
- Torsion-curvature tensor: $\underline{\kappa} = \nabla \underline{\omega}$
- Elasticity: $\underline{\sigma} = \lambda \mathrm{tr}\left(\underline{\underline{\varepsilon}}_e\right) \underline{\underline{I}} + \mu(\underline{\underline{\varepsilon}}_e + \underline{\underline{\varepsilon}}_e^\top) + \mu_c(\underline{\underline{\varepsilon}}_e - \underline{\underline{\varepsilon}}_e^\top), \quad \underline{m} = \alpha \mathrm{tr}\left(\underline{\kappa}_e\right) \underline{\underline{I}} + 2\beta \underline{\kappa}_e$

  $$\boxed{l_e = \sqrt{\beta/\mu}}$$

  Note: $\underline{\underline{\varepsilon}}^\top \neq \underline{\underline{\varepsilon}}, \underline{\kappa}^\top \neq \underline{\kappa}, \underline{\underline{\sigma}}^\top \neq \underline{\underline{\sigma}}, \underline{\underline{m}}^\top \neq \underline{\underline{m}}$
- In non-inertial problems without volume forces and couple-forces, balance of momentum and of moment of momentum:

  $$\nabla \cdot \underline{\underline{\sigma}} = 0, \quad \nabla \cdot \underline{\underline{m}} - {}^3\underline{\underline{\epsilon}} : \underline{\underline{\sigma}} = 0$$
- Plasticity: equivalent stress[1,2] $Y = \sqrt{\frac{3}{2}\left(a_1 \underline{\underline{s}} : \underline{\underline{s}} + a_2 \underline{\underline{s}} : \underline{\underline{s}}^\top + \boxed{\frac{1}{l_p^2}} \underline{\underline{m}} : \underline{\underline{m}}\right)}$
- Internal lengths: elastic l_e, plastic l_p

[1] R. de Borst, L.J. Sluys, *Comp Meth Appl Mech Engin* (1991)
[2] S. Forest, R. Sievert, *Acta Mech* (2003)

---

where permutation tensor ${}^3\underline{\underline{\epsilon}} \sim \epsilon_{ijk} = \begin{cases} 1, & \text{if } \{ijk\} = \{123\} \text{ or } \{231\} \text{ or } \{312\} \\ -1, & \text{if } \{ijk\} = \{321\} \text{ or } \{213\} \text{ or } \{132\} \\ 0, & \text{otherwise} \end{cases}$

Single asperity analysis

Assumptions

- Rigid spherical asperity
- Axisymmetric FE problem
- Generalized Cosserat continuum

Parameters

- Au: $E = 96$ GPa, $\nu = 0.42$, $\sigma_y = 140$ MPa
- $\mu_c = 10\mu, l_e = 100$ nm, $a_1 = 1$
- Indenter radius
  $R \in [0.002, 2000]$ μm

Objectives

- Study size effect
- Enhance asperity based models for rough contact

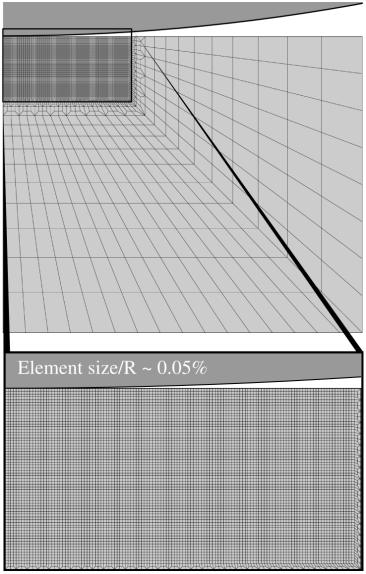

Accumulated plasticity

- Different plastic distribution

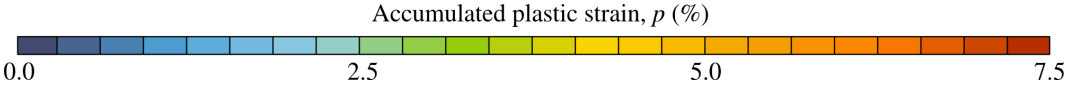

Indenter radius $R = 20\mu$m
Max plastic strain $p_{\max} \approx 7.5\%$

Indenter radius $R = 2\mu$m
Max plastic strain $p_{\max} \approx 11\%$

Accumulated plasticity

- Different plastic distribution

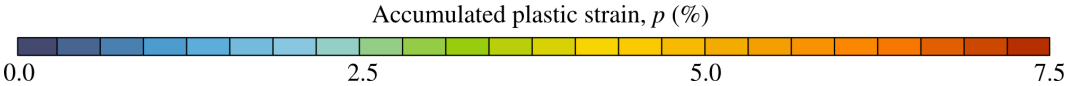

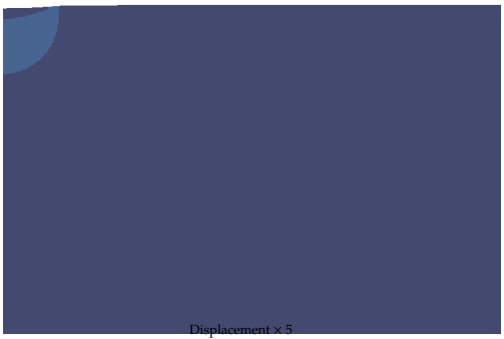

Indenter radius $R = 20\mu$m
Max plastic strain $p_{\max} \approx 7.5\%$

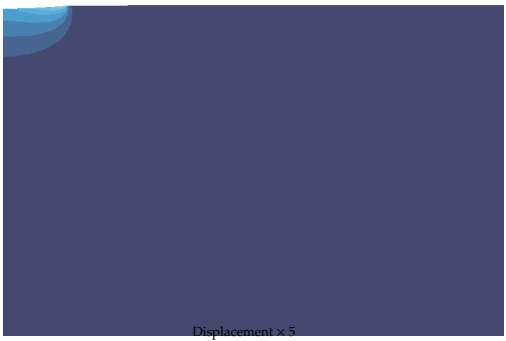

Indenter radius $R = 2\mu$m
Max plastic strain $p_{\max} \approx 11\%$

Accumulated plasticity

- Different plastic distribution

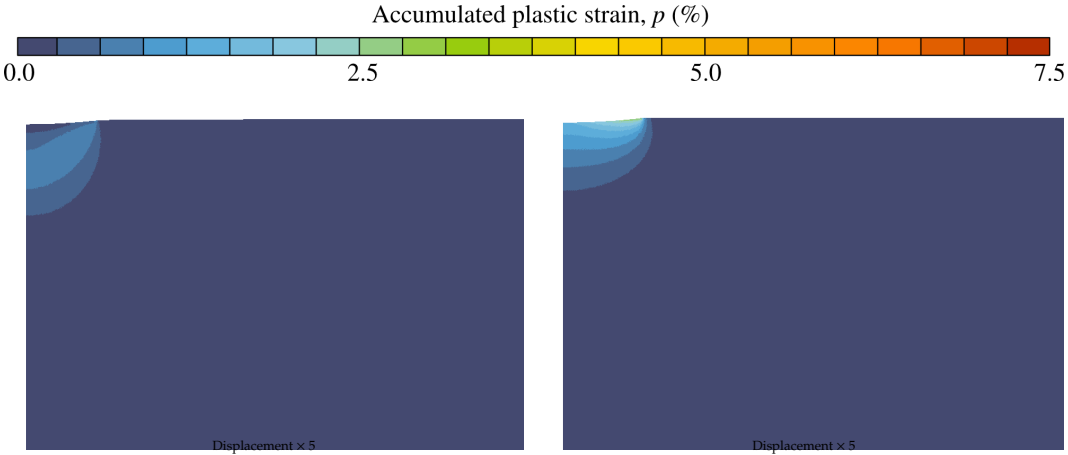

Indenter radius $R = 20\mu$m
Max plastic strain $p_{\max} \approx 7.5\%$

Indenter radius $R = 2\mu$m
Max plastic strain $p_{\max} \approx 11\%$

Accumulated plasticity

- Different plastic distribution

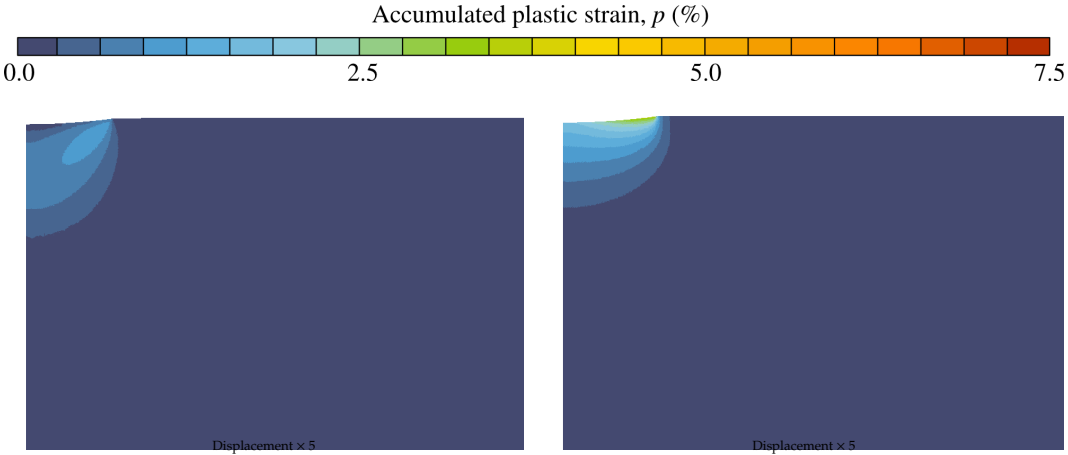

Indenter radius $R = 20\mu$m
Max plastic strain $p_{\max} \approx 7.5\%$

Indenter radius $R = 2\mu$m
Max plastic strain $p_{\max} \approx 11\%$

Accumulated plasticity

- Different plastic distribution

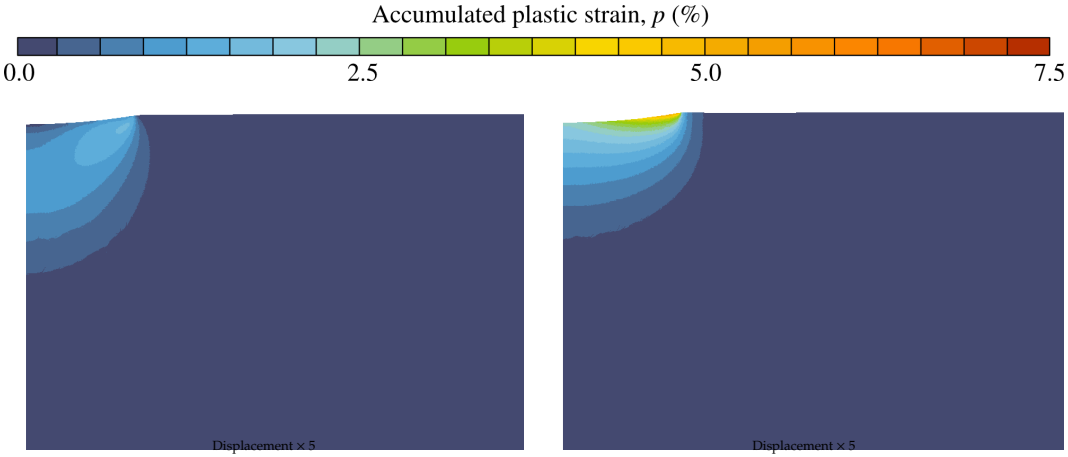

Indenter radius $R = 20\mu$m
Max plastic strain $p_{\max} \approx 7.5\%$

Indenter radius $R = 2\mu$m
Max plastic strain $p_{\max} \approx 11\%$

Accumulated plasticity

- Different plastic distribution

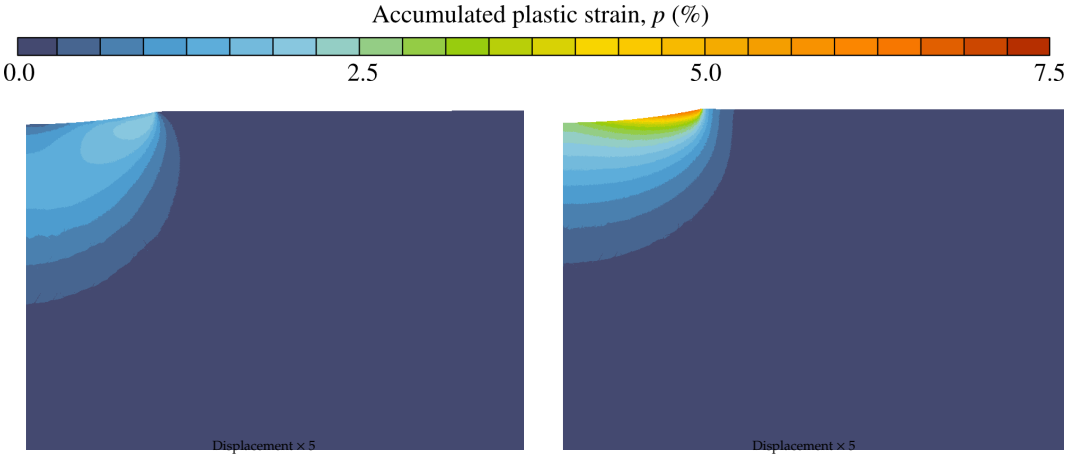

Indenter radius $R = 20\mu$m
Max plastic strain $p_{\max} \approx 7.5\%$

Indenter radius $R = 2\mu$m
Max plastic strain $p_{\max} \approx 11\%$

Accumulated plasticity

- Different plastic distribution

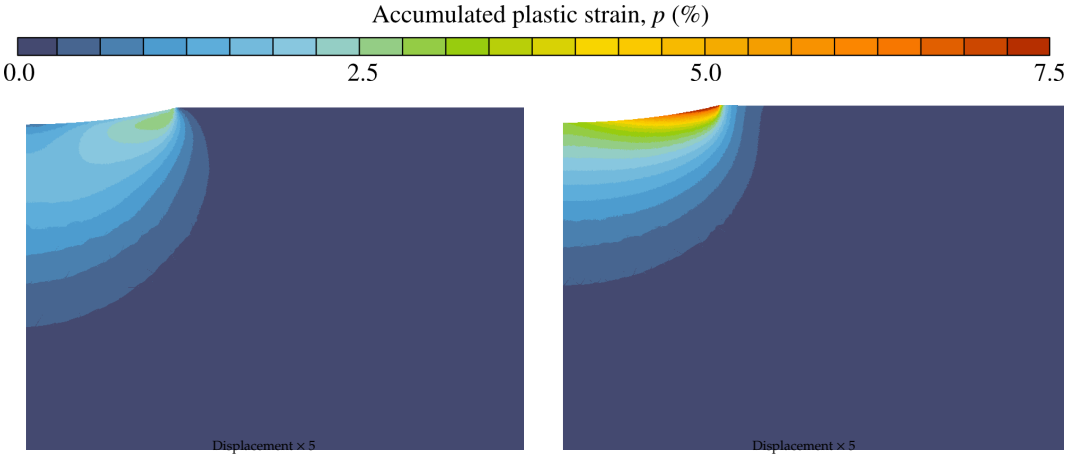

Indenter radius $R = 20\mu$m
Max plastic strain $p_{\max} \approx 7.5\%$

Indenter radius $R = 2\mu$m
Max plastic strain $p_{\max} \approx 11\%$

Accumulated plasticity

- Different plastic distribution

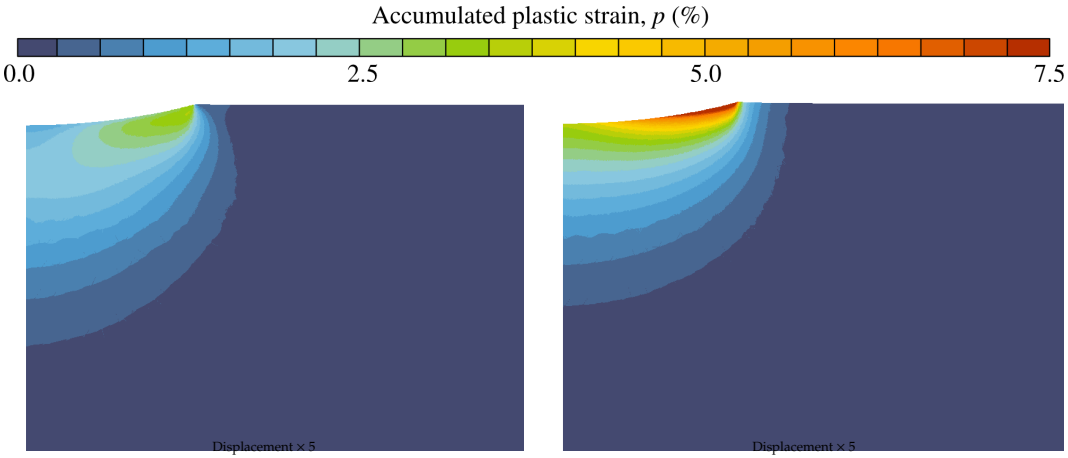

Indenter radius $R = 20\mu$m
Max plastic strain $p_{\max} \approx 7.5\%$

Indenter radius $R = 2\mu$m
Max plastic strain $p_{\max} \approx 11\%$

Accumulated plasticity

- Different plastic distribution

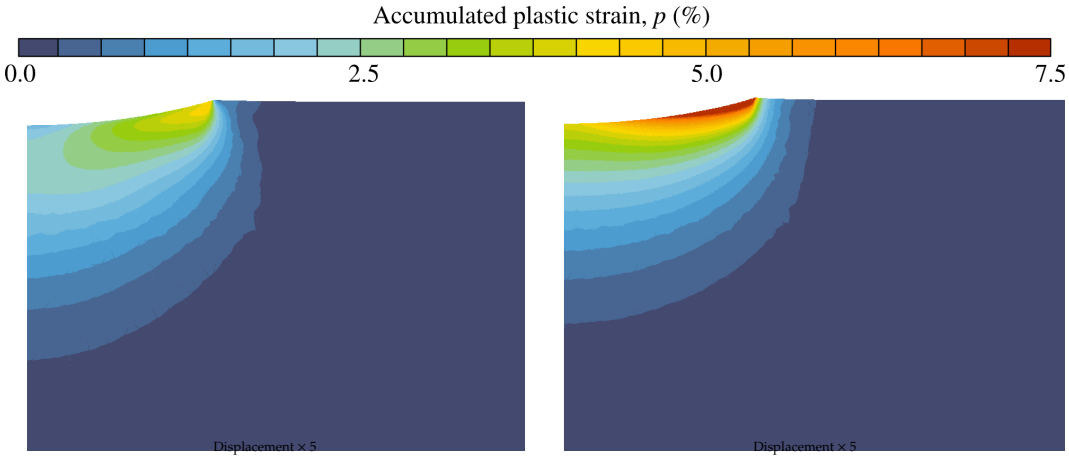

Indenter radius $R = 20\mu$m
Max plastic strain $p_{\max} \approx 7.5\%$

Indenter radius $R = 2\mu$m
Max plastic strain $p_{\max} \approx 11\%$

Displacement–force–contact radius

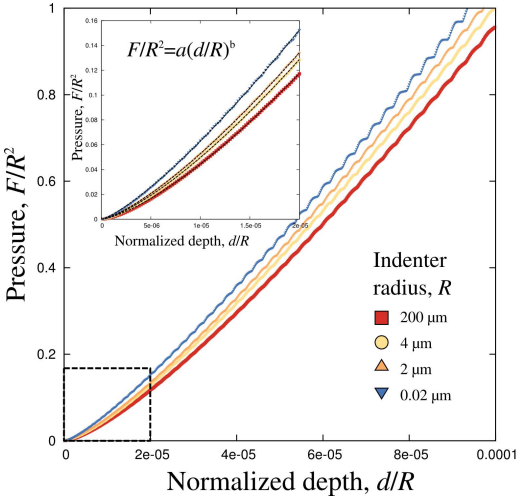

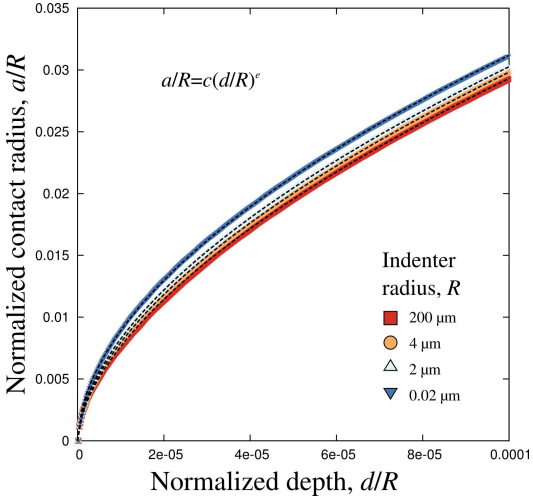

Working model

- Gradient-enhanced hardening with the Cosserat crystal plasticity theory[1]
- Cubic elasticity with C_{11}, C_{12}, C_{44} is to be taken into account

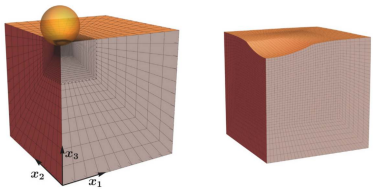

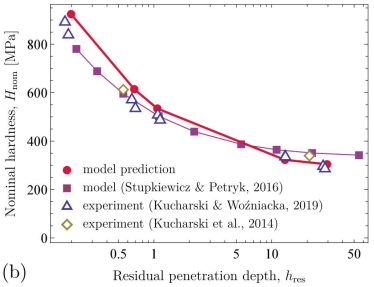

[1] Ryś, M., Stupkiewicz, S. and Petryk, H., 2022. Micropolar regularization of crystal plasticity with the gradient-enhanced incremental hardening law. International Journal of Plasticity, 156, p.103355.

Working model

- Gradient-enhanced hardening with the Cosserat crystal plasticity theory[1]
- Cubic elasticity with C_{11}, C_{12}, C_{44} is to be taken into account

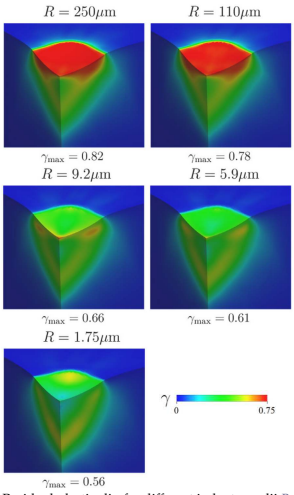

Residual plastic slip for different indenter radii R

[1] Ryś, M., Stupkiewicz, S. and Petryk, H., 2022. Micropolar regularization of crystal plasticity with the gradient-enhanced incremental hardening law. International Journal of Plasticity, 156, p.103355.

Viscoelasticity

One-dimensional constitutive equations

- Applied stress σ
- In the left branch $\sigma_1 = E_\infty \varepsilon$
- In the dashpot $\sigma_2 = \eta \dot{\varepsilon}_d \quad (*)$
- In the right spring $\sigma_2 = E(\varepsilon - \varepsilon_d) \quad (**)$
- For the whole system $\sigma = \sigma_1 + \sigma_2$

$$\boxed{\sigma = (E_\infty + E)\varepsilon - E\varepsilon_d}$$

- From $(*)$ and $(**)$, and denoting $\tau = \eta/E$:

$$\boxed{\dot{\varepsilon}_d = \frac{1}{\tau}\left(\frac{\varepsilon}{\tau} - \varepsilon_d\right)} \qquad \varepsilon_d \xrightarrow[t \to -\infty]{} 0$$

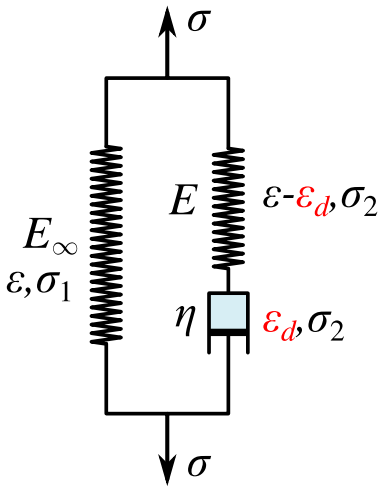

• One-dimensional viscoelastic model

- Multiple dashpots in parallel

$$\sigma = \underbrace{(E_\infty + \sum_i E_i)\varepsilon}_{\text{elastic stress } \sigma_0} - \sum_i E_i \varepsilon_d^i, \quad \dot{\varepsilon}_d^i = \frac{1}{\tau_i}\left(\varepsilon - \varepsilon_d^i\right), \quad \varepsilon_d^i \xrightarrow[t\to-\infty]{} 0, \quad \tau_i = \frac{\eta_i}{E_i}$$

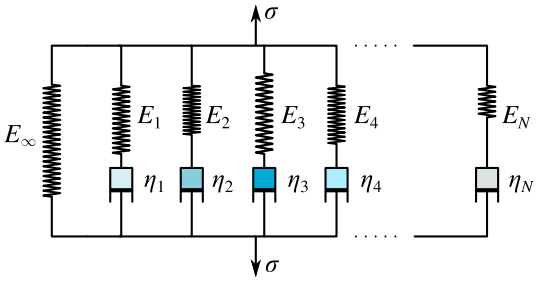

• One-dimensional viscoelastic model

- Multiple dashpots in parallel

$$\sigma = \underbrace{(E_\infty + \sum_i E_i)\varepsilon}_{\text{elastic stress } \sigma_0} - \sum_i E_i \varepsilon_d^i, \quad \dot{\varepsilon}_d^i = \frac{1}{\tau_i}\left(\varepsilon - \varepsilon_d^i\right), \quad \varepsilon_d^i \xrightarrow[t\to-\infty]{} 0, \quad \tau_i = \frac{\eta_i}{E_i}$$

- Denote $E_0 = E_\infty + \sum_i E_i$, $\psi_i = E_i/E_0$, and $q_i = E_i\varepsilon_d^i$ we obtain

$$\sigma = E_0\varepsilon - \sum_i q_i, \quad \dot{q}_i + \frac{q_i}{\tau_i} = \frac{\psi_i}{\tau_i}\sigma_0, \quad \varepsilon_d^i \xrightarrow[t\to-\infty]{} 0$$

- By construction

$$\sum_i \psi_i + \frac{E_\infty}{E_0} = 1 \quad \Rightarrow \quad \sum_i \psi_i = 1 - \frac{E_\infty}{E_0}$$

• Three-dimensional viscoelastic model

Linear viscoelastic (generalized Maxwell model, standard solid)

- Stress-strain relation:

$$\underline{\underline{\sigma}}(t) = K\theta\underline{\underline{I}} + \int_{-\infty}^{t} G(t-\tau)\underline{\underline{\dot{e}}}(\tau)d\tau,$$

- Kernel $G(\tau)$ is given by:

$$G(\tau) = 2G_\infty + 2(G_0 - G_\infty)\Psi(\tau) \text{ with } \Psi(\tau) = \sum_{i=1}^{n} \psi_i \exp(-\tau/\tau_i)$$

  - G_∞, G_0 are the slow/fast loading shear moduli, respectively, such that $G_\infty \leq G_0$;
  - K is the bulk modulus, and for elastomers/polymers $K/G_0 \gg 1$;
  - ψ_i are the influence coefficients, such that $\sum_{i=1}^{n} \psi_i = 1$;
  - τ_i are the respective relaxation times.

• Material model: *storage* and loss moduli

- Consider a harmonic (rigid) loading: $\underline{e}(t) = \underline{e}_0 \exp(i\omega t)$
- Split the kernel: $G(t) = 2G_\infty + \tilde{G}(t)$
- Then, the storage modulus (general case):

$$G'(\omega) = 2G_\infty + \omega \int_0^\infty \tilde{G}(\tau) \sin(\omega\tau)\, d\tau$$

- The storage modulus in the framework of the generalized Maxwell model:

$$G'(\omega) = 2G_\infty + 2\omega(G_0 - G_\infty) \sum_{i=1}^{n} \psi_i \int_0^\infty \exp(-\tau/\tau_i) \sin(\omega\tau)\, d\tau$$

$$G'(\omega) = 2G_\infty + 2(G_0 - G_\infty) \sum_{i=1}^{n} \frac{\psi_i \omega^2 \tau_i^2}{1 + \omega^2 \tau_i^2}$$

- Remark:

$$\int \exp(cx) \sin(bx)\, dx = \frac{\exp(cx)}{c^2 + b^2} [c \sin(bx) - b \cos(bx)]$$

• Material model: storage and *loss* moduli

- The loss modulus (general case):

$$G''(\omega) = \omega \int_0^\infty \tilde{G}(\tau) \cos(\omega\tau)\, d\tau$$

- The loss modulus in the framework of the generalized Maxwell model:

$$G''(\omega) = 2\omega(G_0 - G_\infty) \sum_{i=1}^{n} \psi_i \int_0^\infty \exp(-\tau/\tau_i) \cos(\omega\tau)\, d\tau$$

$$G''(\omega) = 2(G_0 - G_\infty) \sum_{i=1}^{n} \frac{\psi_i \omega\tau_i}{1 + \omega^2\tau_i^2}.$$

- Remark:

$$\int \exp(cx) \cos(bx)\, dx = \frac{\exp(cx)}{c^2 + b^2}[c\cos(bx) + b\sin(bx)]$$

• Material model: example

- Material parameters: $G_0 = 1.1$ MPa, $G_\infty = 50$ kPa
- Single relaxation time: $\tau_0 = 10^{-7}$ s
- Quasi-incompressible material: $K/G_0 = 10^6 \gg 1$
- Uniaxial (rigid) loading: $\varepsilon_{xx} = A\sin(\omega t)$, $\sigma_{yy} = \sigma_{zz} = 0$, $\varepsilon_{yy} = \varepsilon_{zz} \approx -0.5\varepsilon_{xx}$
- Spherical and deviatoric parts: $\underline{\boldsymbol{\epsilon}} \approx A(1-2\nu)\sin(\omega t)\underline{\boldsymbol{I}}$, $\underline{\boldsymbol{e}} \approx \underline{\boldsymbol{\varepsilon}}$
- Stress-strain relation: $\underline{\boldsymbol{\sigma}}(t) = \int_{-\infty}^{t} 2(G_0 - G_\infty)\exp[-(t-\tau)/\tau_0]\underline{\dot{\boldsymbol{e}}}(\tau)d\tau + 2G_\infty\underline{\boldsymbol{e}} + K\underline{\boldsymbol{\epsilon}}$,
- Axial and radial stress components:

$$\sigma_{xx} = 2G_\infty\varepsilon_{xx} + K(\varepsilon_{xx} + 2\varepsilon_{yy}) + \int_{-\infty}^{t} 2(G_0 - G_\infty)\exp[-(t-\tau)/\tau_0]\dot{\varepsilon}_{xx}(\tau)d\tau$$

• Material model: example

- Material parameters: $G_0 = 1.1$ MPa, $G_\infty = 50$ kPa
- Single relaxation time: $\tau_0 = 10^{-7}$ s
- Quasi-incompressible material: $K/G_0 = 10^6 \gg 1$
- Uniaxial (rigid) loading: $\varepsilon_{xx} = A\sin(\omega t)$, $\sigma_{yy} = \sigma_{zz} = 0$, $\varepsilon_{yy} = \varepsilon_{zz} \approx -0.5\varepsilon_{xx}$
- Spherical and deviatoric parts: $\underline{\boldsymbol{\epsilon}} \approx A(1-2\nu)\sin(\omega t)\underline{\boldsymbol{I}}$, $\underline{\boldsymbol{e}} \approx \underline{\boldsymbol{\varepsilon}}$
- Stress-strain relation: $\underline{\boldsymbol{\sigma}}(t) = \int\limits_{-\infty}^{t} 2(G_0 - G_\infty)\exp[-(t-\tau)/\tau_0]\underline{\dot{\boldsymbol{e}}}(\tau)d\tau + 2G_\infty\underline{\boldsymbol{e}} + K\underline{\boldsymbol{\epsilon}}$,
- Axial and radial stress components:

$$\sigma_{xx} = 2G_\infty\varepsilon_{xx} + K(\varepsilon_{xx} + 2\varepsilon_{yy}) + \int\limits_{-\infty}^{t} 2(G_0 - G_\infty)\exp[-(t-\tau)/\tau_0]\dot{\varepsilon}_{xx}(\tau)d\tau$$

$$\sigma_{yy} = 0$$

• Material model: example

- Material parameters: $G_0 = 1.1$ MPa, $G_\infty = 50$ kPa
- Single relaxation time: $\tau_0 = 10^{-7}$ s
- Quasi-incompressible material: $K/G_0 = 10^6 \gg 1$
- Uniaxial (rigid) loading: $\varepsilon_{xx} = A\sin(\omega t)$, $\sigma_{yy} = \sigma_{zz} = 0$, $\varepsilon_{yy} = \varepsilon_{zz} \approx -0.5\varepsilon_{xx}$
- Spherical and deviatoric parts: $\underline{\boldsymbol{\epsilon}} \approx A(1-2\nu)\sin(\omega t)\underline{\boldsymbol{I}}$, $\underline{\boldsymbol{e}} \approx \underline{\boldsymbol{\varepsilon}}$
- Stress-strain relation: $\underline{\boldsymbol{\sigma}}(t) = \int_{-\infty}^{t} 2(G_0 - G_\infty)\exp[-(t-\tau)/\tau_0]\underline{\dot{\boldsymbol{e}}}(\tau)d\tau + 2G_\infty\underline{\boldsymbol{e}} + K\underline{\boldsymbol{\epsilon}}$,
- Axial and radial stress components:

$$\sigma_{xx} = 2G_\infty\varepsilon_{xx} + K(\varepsilon_{xx} + 2\varepsilon_{yy}) + \int_{-\infty}^{t} 2(G_0 - G_\infty)\exp[-(t-\tau)/\tau_0]\dot{\varepsilon}_{xx}(\tau)d\tau$$

$$\sigma_{yy} = 0 = 2G_\infty\varepsilon_{yy} + K(\varepsilon_{xx} + 2\varepsilon_{yy}) + \int_{-\infty}^{t} 2(G_0 - G_\infty)\exp[-(t-\tau)/\tau_0]\dot{\varepsilon}_{yy}(\tau)d\tau$$

• Material model: example

- Material parameters: $G_0 = 1.1$ MPa, $G_\infty = 50$ kPa
- Single relaxation time: $\tau_0 = 10^{-7}$ s
- Quasi-incompressible material: $K/G_0 = 10^6 \gg 1$
- Uniaxial (rigid) loading: $\varepsilon_{xx} = A\sin(\omega t)$, $\sigma_{yy} = \sigma_{zz} = 0$, $\varepsilon_{yy} = \varepsilon_{zz} \approx -0.5\varepsilon_{xx}$
- Spherical and deviatoric parts: $\underline{\boldsymbol{\epsilon}} \approx A(1-2\nu)\sin(\omega t)\underline{\boldsymbol{I}}$, $\underline{\boldsymbol{e}} \approx \underline{\boldsymbol{\varepsilon}}$
- Stress-strain relation: $\underline{\boldsymbol{\sigma}}(t) = \int\limits_{-\infty}^{t} 2(G_0 - G_\infty)\exp[-(t-\tau)/\tau_0]\underline{\dot{\boldsymbol{e}}}(\tau)d\tau + 2G_\infty\underline{\boldsymbol{e}} + K\underline{\boldsymbol{\epsilon}}$,
- Axial and radial stress components:

$$\sigma_{xx} = 2G_\infty\varepsilon_{xx} + K(\varepsilon_{xx} + 2\varepsilon_{yy}) + \int\limits_{-\infty}^{t} 2(G_0 - G_\infty)\exp[-(t-\tau)/\tau_0]\dot{\varepsilon}_{xx}(\tau)d\tau$$

$$\sigma_{yy} = 0 = 2G_\infty\varepsilon_{yy} + K(\varepsilon_{xx} + 2\varepsilon_{yy}) + \int\limits_{-\infty}^{t} 2(G_0 - G_\infty)\exp[-(t-\tau)/\tau_0]\dot{\varepsilon}_{yy}(\tau)d\tau$$

$$\boxed{\sigma_{xx} = 3G_\infty\varepsilon_{xx} + \int\limits_{-\infty}^{t} 3(G_0 - G_\infty)\exp[-(t-\tau)/\tau_0]\dot{\varepsilon}_{xx}(\tau)d\tau}$$

• Material model: example II

- Uniaxial storage modulus:

$$E'(\omega) = 3G_\infty + 3(G_0 - G_\infty)\frac{\omega^2\tau_0^2}{1+\omega^2\tau_0^2}$$

- Uniaxial loss modulus:

$$E''(\omega) = 3(G_0 - G_\infty)\frac{\omega\tau}{1+\omega^2\tau_0^2}$$

• Material model: example (FEA vs Analytics)

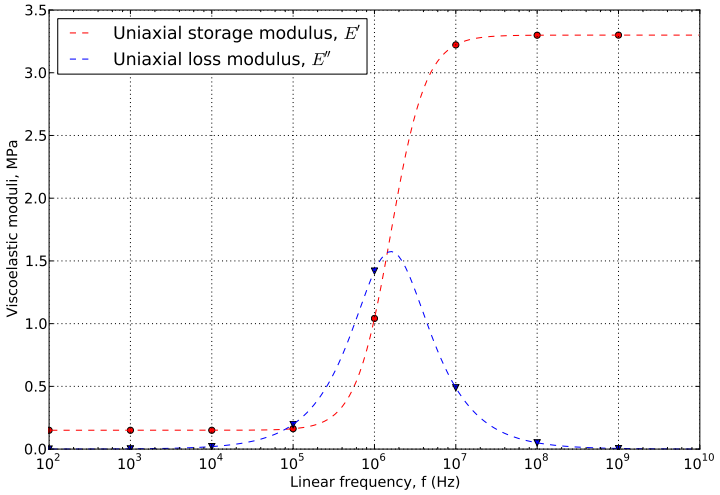

• Material model: example (FEA vs Analytics)

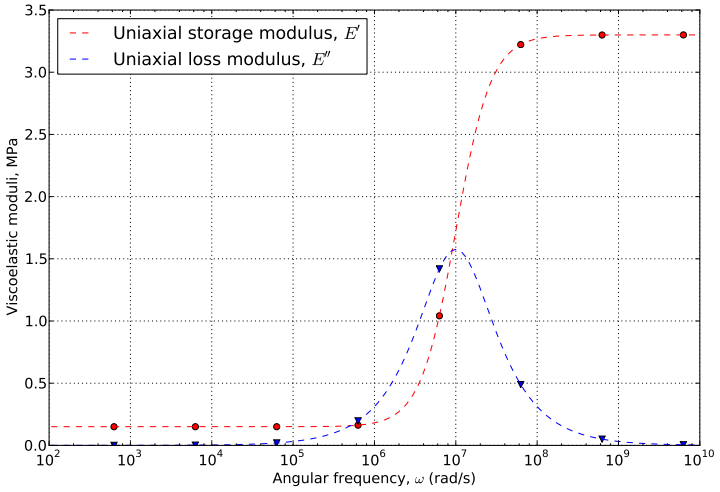

• Material model: example (FEA vs Analytics)

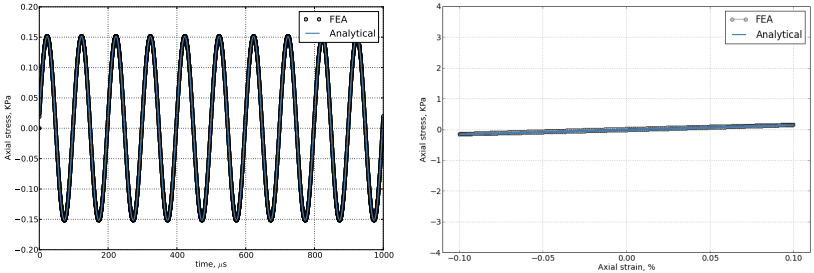

Linear frequency $f = 10^4$ Hz

• Material model: example (FEA vs Analytics)

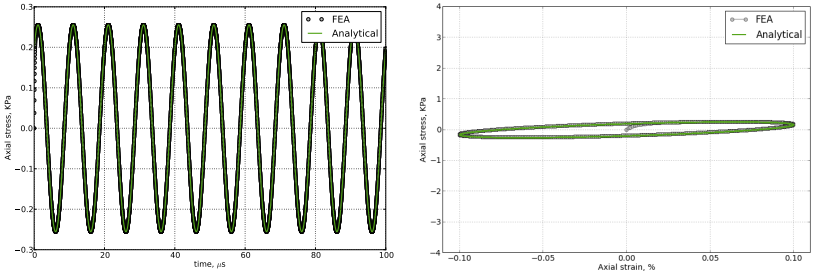

Linear frequency $f = 10^5$ Hz

• Material model: example (FEA vs Analytics)

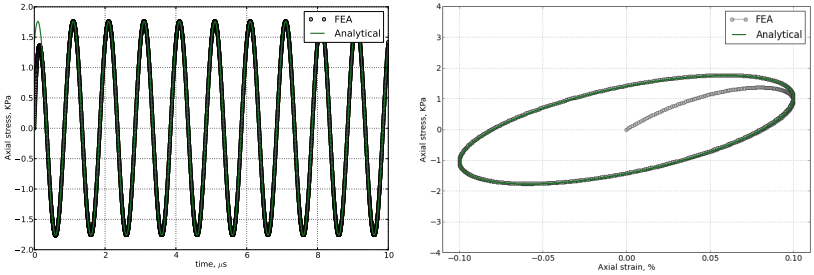

Linear frequency $f = 10^6$ Hz

• Material model: example (FEA vs Analytics)

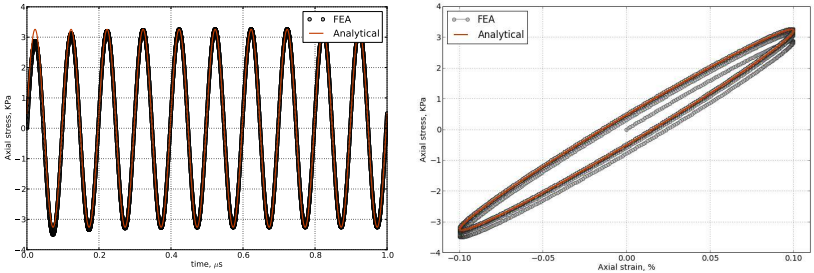

Linear frequency $f = 10^7$ Hz

• Material model: example (FEA vs Analytics)

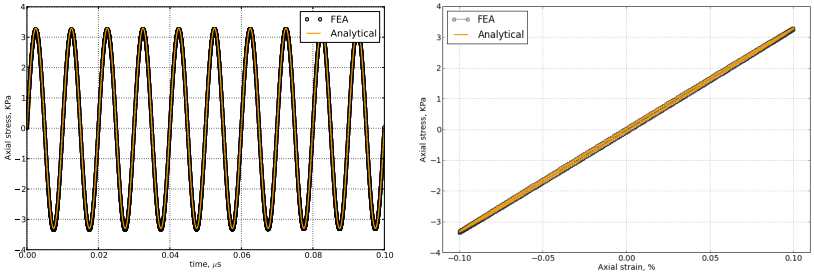

Linear frequency $f = 10^8$ Hz

• Viscoelastic sliding

Viscoelastic sliding: bulk friction

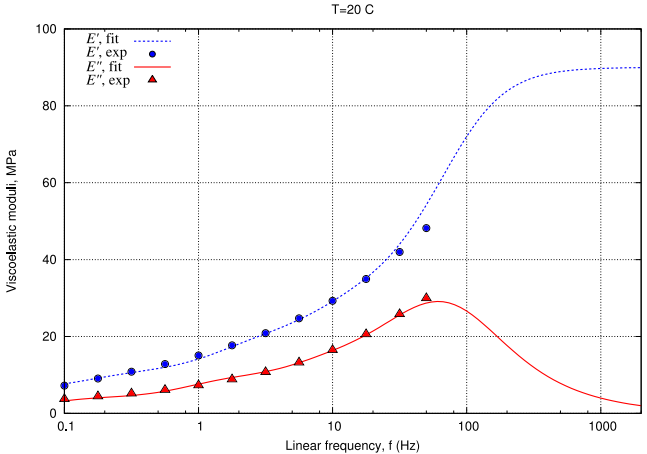

Fitting generalized Maxwell model for rubber to experimental data at T = 20 ^{o}C

Viscoelastic sliding: bulk friction

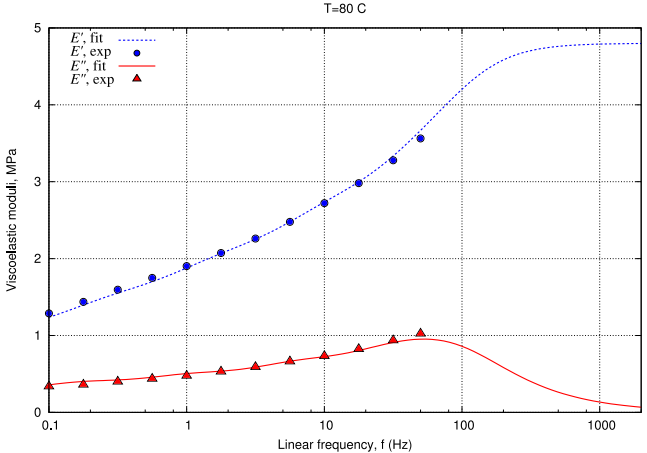

Fitting generalized Maxwell model for rubber to experimental data at T = 80 °C

Viscoelastic sliding: bulk friction

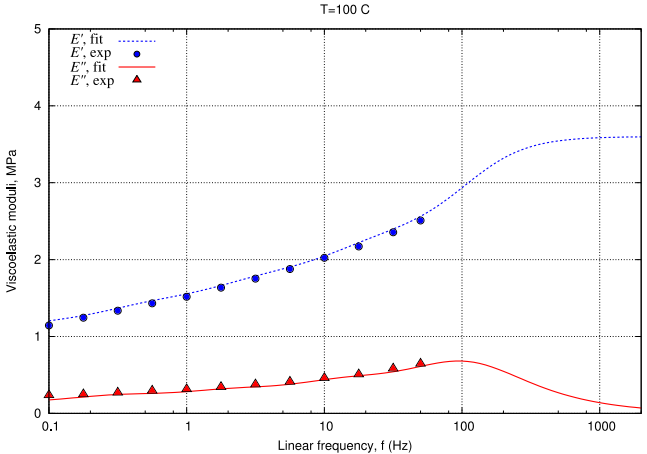

Fitting generalized Maxwell model for rubber to experimental data at T = 100 °C

Viscoelastic sliding: bulk friction

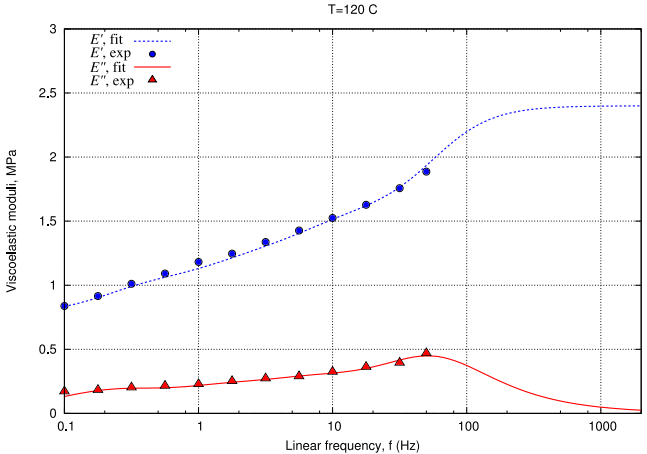

Fitting generalized Maxwell model for rubber to experimental data at T = 120 °C

Viscoelastic sliding: bulk friction

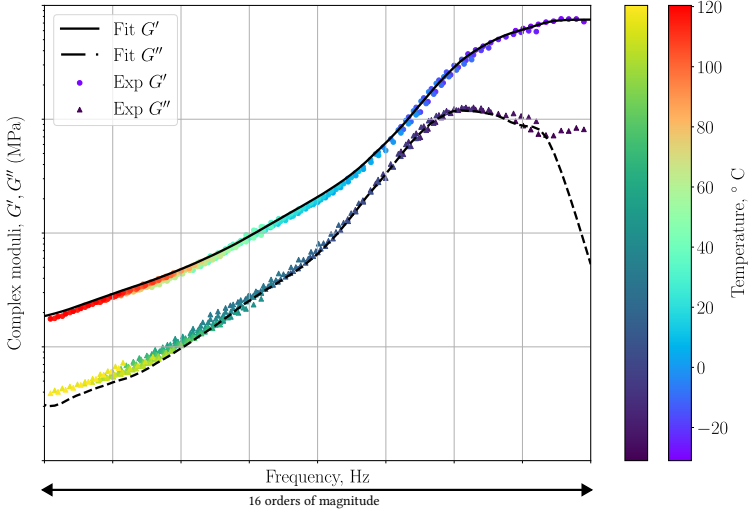

Full data on complex moduli of a sample charged rubber

Viscoelastic sliding: bulk friction

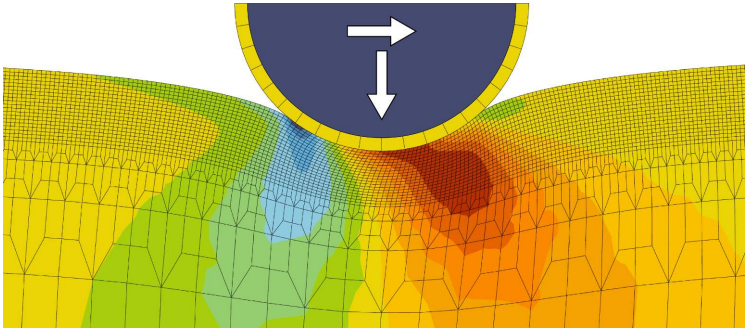

Simulation sketch

Viscoelastic sliding: bulk friction

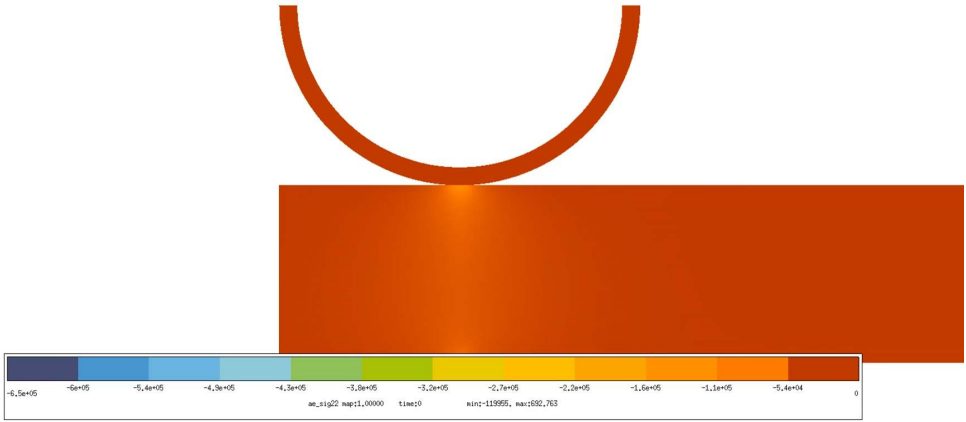

Stress field σ_{yy}

Viscoelastic sliding: bulk friction

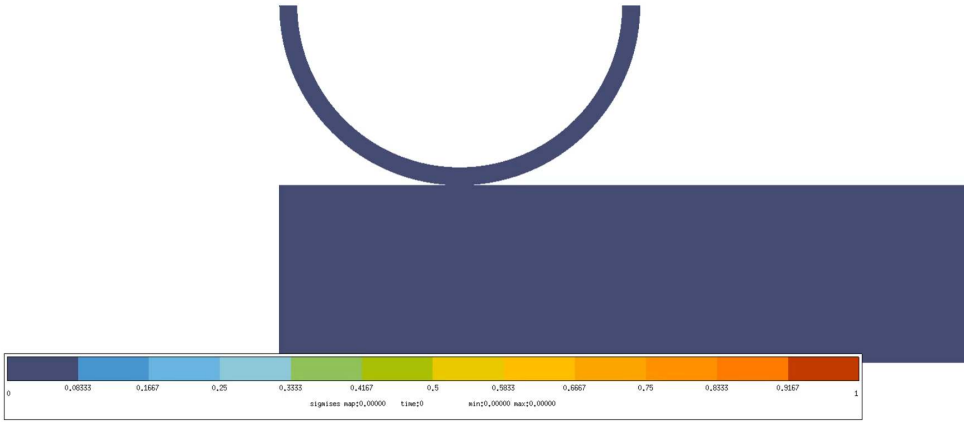

Von Mises stress field

Viscoelastic sliding: bulk friction

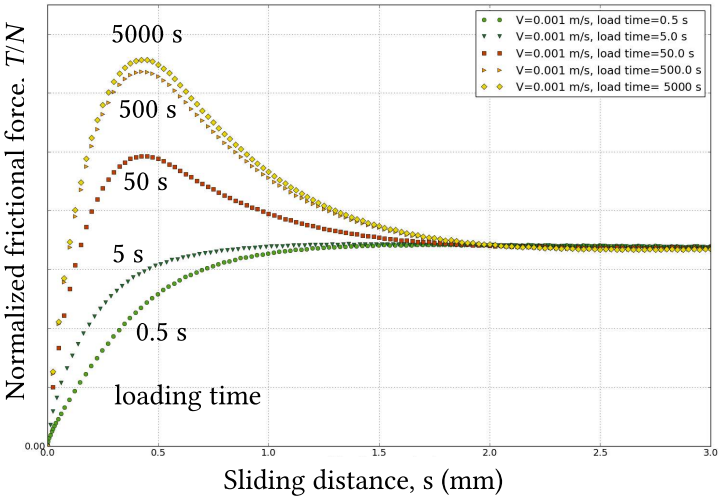

Effect of normal-loading rate on the frictional force evolution

Viscoelastic sliding: bulk friction

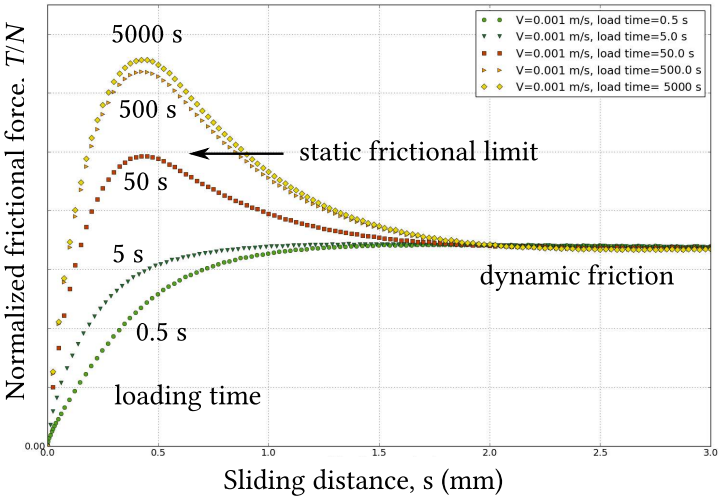

Effect of normal-loading rate on the frictional force evolution

Viscoelastic sliding: bulk friction

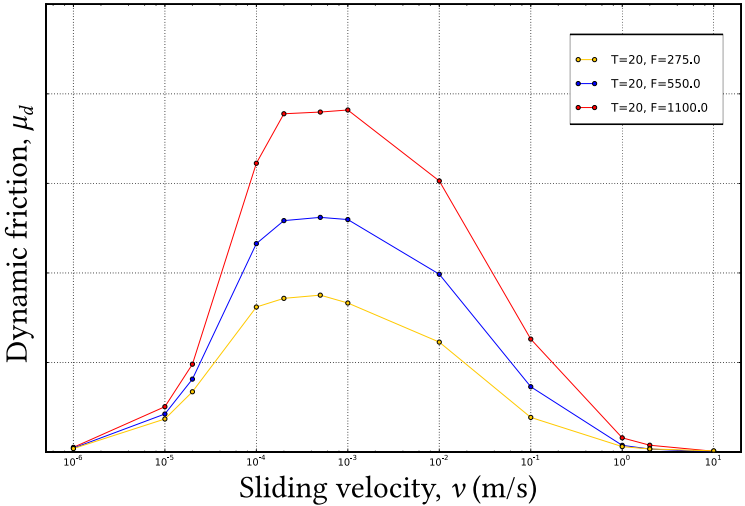

Frictional force at different slip velocity (effect of force)

Viscoelastic sliding: bulk friction

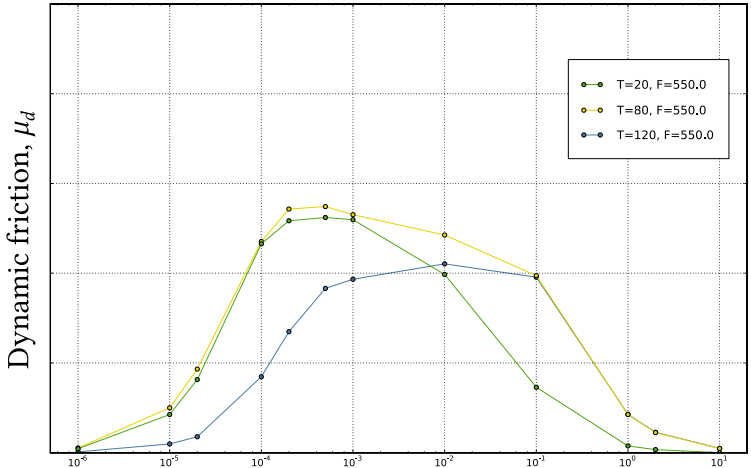

Frictional force at different slip velocity (effect of temperature)

Viscoelastic friction: recent progress

- Account for multiscales[1,2]
- Account for adhesion[1,2]
- Account for large deformations[3]

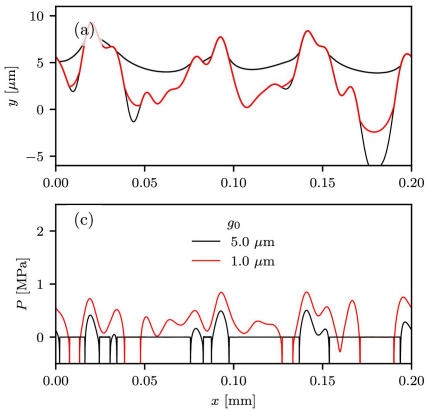

Simulation results[1]

[1] Plagge, J. and Hentschke, R., (2022) Numerical solution of the adhesive rubber-solid contact problem and friction coefficients using a scale-splitting approach. Tribology International, 173:107622.

[2] Carbone, G., Mandriota, C. and Menga, N., (2022) Theory of viscoelastic adhesion and friction. Extreme Mechanics Letters, 56:101877.

[3] Lengiewicz, J., de Souza, M., Lahmar, M.A., Courbon, C., Dalmas, D., Stupkiewicz, S. and Scheibert, J., (2020) Finite deforma- tions govern the anisotropic shear-induced area reduction of soft elastic 2contacts. Journal of the Mechanics and Physics of Solids, 143:104056

Viscoelastic friction: recent progress

- Account for multiscales[1,2]
- Account for adhesion[1,2]
- Account for large deformations[3]

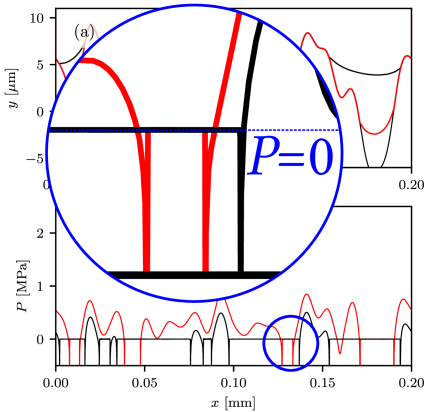

Simulation results[1]

[1] Plagge, J. and Hentschke, R., (2022) Numerical solution of the adhesive rubber-solid contact problem and friction coefficients using a scale-splitting approach. Tribology International, 173:107622.

[2] Carbone, G., Mandriota, C. and Menga, N., (2022) Theory of viscoelastic adhesion and friction. Extreme Mechanics Letters, 56:101877.

[3] Lengiewicz, J., de Souza, M., Lahmar, M.A., Courbon, C., Dalmas, D., Stupkiewicz, S. and Scheibert, J., (2020) Finite deforma- tions govern the anisotropic shear-induced area reduction of soft elastic 2contacts. Journal of the Mechanics and Physics of Solids, 143:104056

Viscoelastic friction: recent progress

- Account for multiscales[1,2]
- Account for adhesion[1,2]
- Account for large deformations[3]

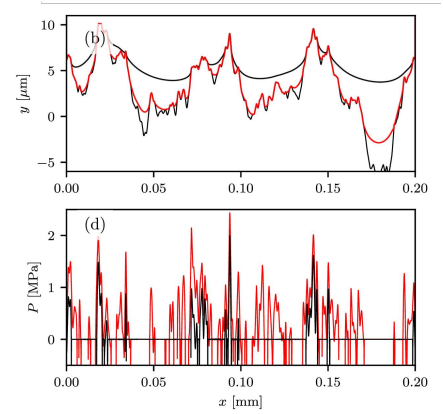

Simulation results[1]

[1] Plagge, J. and Hentschke, R., (2022) Numerical solution of the adhesive rubber-solid contact problem and friction coefficients using a scale-splitting approach. Tribology International, 173:107622.

[2] Carbone, G., Mandriota, C. and Menga, N., (2022) Theory of viscoelastic adhesion and friction. Extreme Mechanics Letters, 56:101877.

[3] Lengiewicz, J., de Souza, M., Lahmar, M.A., Courbon, C., Dalmas, D., Stupkiewicz, S. and Scheibert, J., (2020) Finite deforma- tions govern the anisotropic shear-induced area reduction of soft elastic 2contacts. Journal of the Mechanics and Physics of Solids, 143:104056

Viscoelastic friction: recent progress

- Account for multiscales[1,2]
- Account for adhesion[1,2]
- Account for large deformations[3]

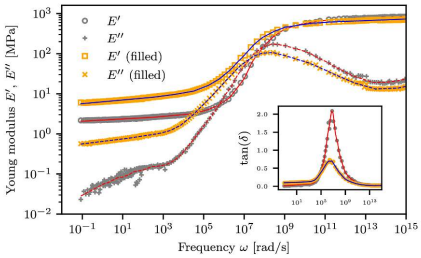

Simulation results[1]

[1] Plagge, J. and Hentschke, R., (2022) Numerical solution of the adhesive rubber-solid contact problem and friction coefficients using a scale-splitting approach. Tribology International, 173:107622.

[2] Carbone, G., Mandriota, C. and Menga, N., (2022) Theory of viscoelastic adhesion and friction. Extreme Mechanics Letters, 56:101877.

[3] Lengiewicz, J., de Souza, M., Lahmar, M.A., Courbon, C., Dalmas, D., Stupkiewicz, S. and Scheibert, J., (2020) Finite deforma- tions govern the anisotropic shear-induced area reduction of soft elastic 2contacts. Journal of the Mechanics and Physics of Solids, 143:104056

Viscoelastic friction: recent progress

- Account for multiscales[1,2]
- Account for adhesion[1,2]
- Account for large deformations[3]

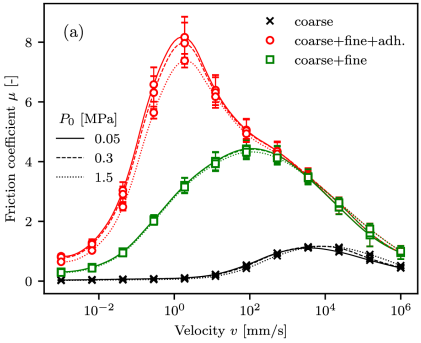

Simulation results[1]

[1] Plagge, J. and Hentschke, R., (2022) Numerical solution of the adhesive rubber-solid contact problem and friction coefficients using a scale-splitting approach. Tribology International, 173:107622.

[2] Carbone, G., Mandriota, C. and Menga, N., (2022) Theory of viscoelastic adhesion and friction. Extreme Mechanics Letters, 56:101877.

[3] Lengiewicz, J., de Souza, M., Lahmar, M.A., Courbon, C., Dalmas, D., Stupkiewicz, S. and Scheibert, J., (2020) Finite deforma- tions govern the anisotropic shear-induced area reduction of soft elastic 2contacts. Journal of the Mechanics and Physics of Solids, 143:104056

Thank you for your attention!